Journal of Theoretical Biology 310 (2012) 143–159

Contents lists available at SciVerse ScienceDirect

Journal of Theoretical Biology

journal homepage: www.elsevier.com/locate/yjtbi

A prototypic mathematical model of the human hair cycle

Yusur Al-Nuaimi [a,b,*,1], Marc Goodfellow [a,c,1], Ralf Paus [b,d], Gerold Baier [a]

[a] Doctoral Training Centre in Integrative Systems Biology, Manchester Interdisciplinary Biocentre, University of Manchester, UK
[b] Inflammation Sciences, School of Translational Medicine, Manchester Academic Health Sciences Centre, University of Manchester, UK
[c] Centre for Interdisciplinary Computational and Dynamical Analysis (CICADA), Alan Turing Building, University of Manchester, UK
[d] Department of Dermatology, University of Lübeck, Germany

HIGHLIGHTS

- We model normal human hair follicle oscillations and its abnormalities.
- Interaction between two compartments is essential for hair cycling.
- Hair follicle cycling arises from spontaneous switching between a no growth and a growth state.
- Bistability and excitability are studied in the context of pathological states.
- The model is a prototype for further mechanistic study of hair follicle dynamics.

ARTICLE INFO

Article history:
Received 12 November 2011
Received in revised form
21 May 2012
Accepted 25 May 2012
Available online 4 June 2012

Keywords:
Systems biology
Compartment model
Hair follicle oscillations
Bistability
Excitability

ABSTRACT

The human hair cycle is a complex, dynamic organ-transformation process during which the hair follicle repetitively progresses from a growth phase (anagen) to a rapid apoptosis-driven involution (catagen) and finally a relative quiescent phase (telogen) before returning to anagen. At present no theory satisfactorily explains the origin of the hair cycle rhythm. Based on experimental evidence we propose a prototypic model that focuses on the dynamics of hair matrix keratinocytes. We argue that a plausible feedback-control structure between two key compartments (matrix keratinocytes and dermal papilla) leads to dynamic instabilities in the population dynamics resulting in rhythmic hair growth. The underlying oscillation consists of an autonomous switching between two quasi-steady states. Additional features of the model, namely bistability and excitability, lead to new hypotheses about the impact of interventions on hair growth. We show how *in silico* testing may facilitate testing of candidate hair growth modulatory agents in human HF organ culture or in clinical trials.

1. Introduction

The hair follicle (HF) is unique to mammals and displays fascinating dynamic behaviour in the hair cycle. This cutaneous mini-organ undergoes continuous, self-organised, cyclical regeneration and regression events during which a pigmented hair shaft is produced and shed during each cycle (Fig. 1). The hair cycle is the only organ transformation event that repeats cyclically for the entire lifetime of the mammalian individual. It represents a unique chronobiological rhythm that encompasses a complex set of changes at the tissue level. In addition, it shows diverse rhythmicity, dependent on where on the integument a HF is located (e.g. scalp versus eyelashes versus eyebrow hair) (Dawber, 1997). The "control" system that governs the hair cycle is proposed to be an autonomous oscillator (Paus et al., 1999; Paus and Foitzik, 2004). Its exact molecular constituents and operation principles, however, have essentially remained elusive.

HF cycling commences immediately after HF morphogenesis (Fig. 1) and consists of three main phases: anagen, a phase of massive epithelial cell proliferation, during which pigmented hair shafts are generated in the anagen hair bulb; catagen, a phase of rapid, apoptosis-driven organ involution; and telogen, an interspersed stage of relative quiescence (Stenn and Paus, 2001; Paus and Foitzik, 2004; Schneider et al., 2009) (Fig. 1). Active hair shaft shedding occurs during exogen (Milner et al., 2002; Higgins et al., 2009). Each phase in the cycle is of distinct length (e.g. with anagen lasting several years, catagen several weeks, and telogen usually a few months in human scalp HFs). All human HFs show

Abbreviations: HF, hair follicle; MK, matrix keratinocytes; DP, dermal papilla; CTS, connective tissue sheath; HFPU, hair follicle pigmentary unit; TAC, transient amplifying cell; IRS, inner root sheath; ORS, outer root sheath; MC, melanocytes; HSC, hair stem cells; APM, arrector pili muscle; DC, dermal condensate; SC, sebocytes; SG, sebaceous gland

* Correspondence to: Yusur Al-Nuaimi, Academic Clinical Fellow in Dermatology, Academic Health Sciences Centre, Room 2.202a, Stopford Building, University of Manchester, Oxford Road, Manchester M13 9PT, UK. Tel.: +44 7876440446.
E-mail address: yusur.al-nuaimi@manchester.ac.uk (Y. Al-Nuaimi).

[1] These authors contributed equally.

0022-5193/$ - see front matter © 2012 Elsevier Ltd. All rights reserved.
http://dx.doi.org/10.1016/j.jtbi.2012.05.027

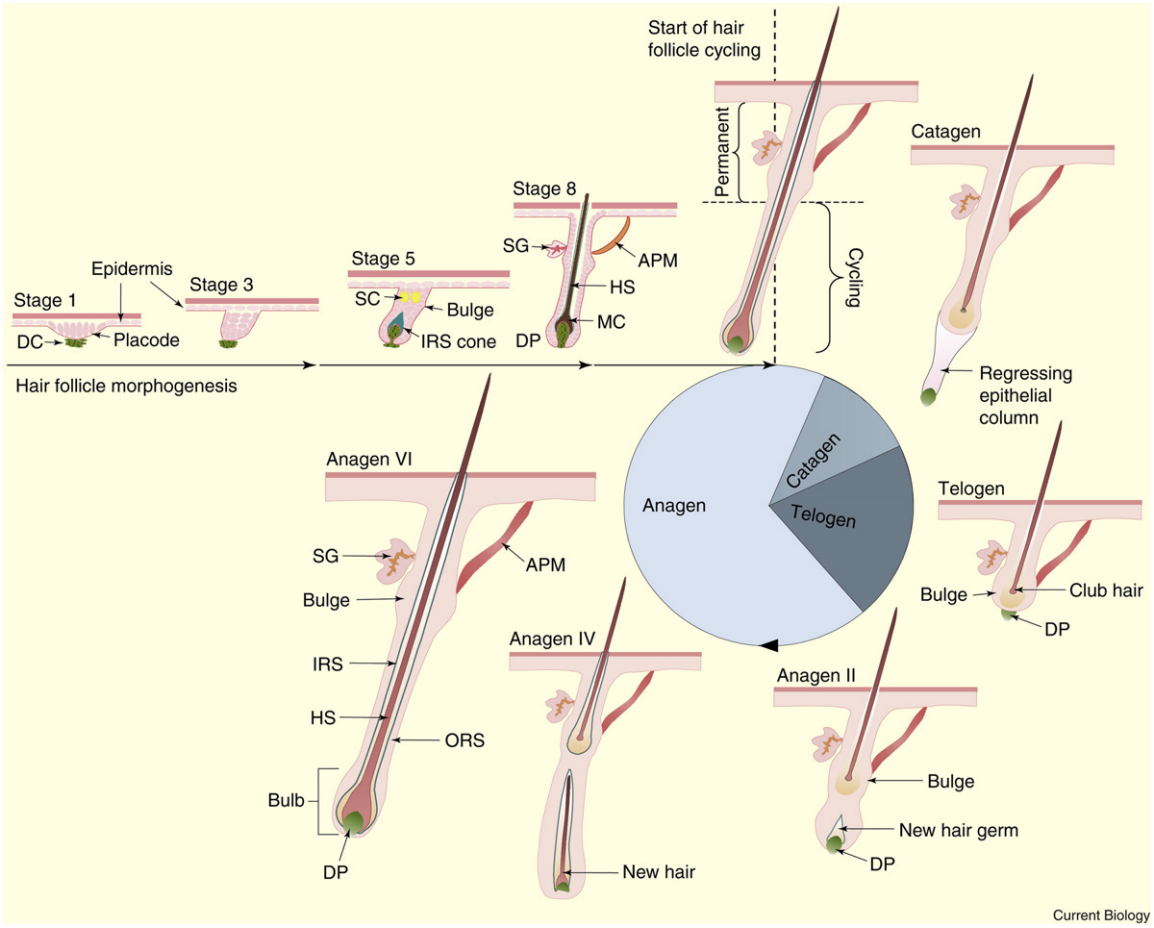

Fig. 1. Key stages of the hair cycle. The hair cycle is divided into three phases: Anagen (growth phase), catagen (regression phase) and telogen (resting phase). Hair follicle morphogenesis leads to elongation of the follicle and production of the hair fibre, which emerges from the skin. Once the hair follicle has matured, it enters the regression phase (catagen), during which the lower, cycling portion of the hair follicle is degraded. This process brings the dermal papilla into close proximity of the bulge, where the hair stem cells (HSC) reside. The proximity between bulge and dermal papilla is maintained throughout telogen, the resting phase. Only when a critical concentration of hair growth activating signals is reached, anagen phase is entered and a new hair is regrown. Stages 1–8 of embryonic hair development are depicted (upper left), demonstrating the continuous transition between hair follicle development and the first hair cycle. APM: arrector pili muscle; DC, dermal condensate (green); DP: dermal papilla (green); HS: hair shaft (brown); IRS: inner root sheath (blue); MC: melanocytes; ORS: outer root sheath; SC: sebocytes (yellow); SG: sebaceous gland. (Reproduced and adapted after Schneider et al., 2009 with permission.) (For interpretation of the references to color in this figure legend, the reader is referred to the web version of this article.)

major site-specific variations in the length of each of these phases (Kligman, 1959; Saitoh et al., 1970).

Hair cycling is of clinical relevance as the majority of hair disorders are characterised by a pathological change in normal HF cycling dynamics (Cotsarelis and Millar, 2001; Paus, 2006). If anagen is abrogated and catagen induced prematurely this will result in hair loss (effluvium). In contrast, when anagen is induced prematurely or lasts overly long, this leads to unwanted hair growth (hirsutism, hypertrichosis). In addition, dramatic transformations in HF size and state can occur during just one hair cycle, which may underlie the HF transformation events seen when very small (vellus) HFs become large, or very large HF miniaturise during hirsutism, hypertrichosis or androgenetic alopecia, respectively (Stenn and Paus, 2001; Tobin et al., 2003; Paus and Foitzik, 2004; Schneider et al., 2009).

Over the years, a multitude of genes, secreted molecules, enzymes and receptors have been identified that modulate HF cycling, hair shaft growth and hair pigmentation (Stenn et al., 1994; Stenn and Paus, 2001; Plikus et al., 2009; Schneider et al., 2009; Geyfman and Andersen, 2010). An emerging general consensus is that controlled changes in the expression, secretion or activity of these molecules leads to switches in the local signalling environment, which ultimately drive the HF through its cyclic transformations (Paus and Foitzik, 2004; Schneider et al., 2009). However, we remain unsure of the "pacemaker(s)" that autonomously govern the coordinated and timely progression of the whole organ through the hair cycle (Paus et al., 1999; Paus and Foitzik, 2004).

1.1. *The "hair cycle clock": a modelling challenge*

The need to explain the origin of HF cycling was first systematically addressed over half a century ago by Chase who proposed an inhibition-disinhibition theory of how the hair cycle rhythm arises (Chase, 1954). This theory postulated the gradual build-up in activity of an inhibitor during active hair growth (anagen), which would eventually switch anagen off once a certain threshold had been reached; hair growth would become reactivated ("disinhibited") as the activity of the inhibitor had spontaneously declined again. While this elegant theory has received limited experimental support (Paus et al., 1990) it remains to be rigorously followed-up. More recently, this theoretical challenge has been re-examined as an important, and as yet unanswered, biological problem of general importance (Paus et al., 1999; Stenn et al., 1999; Paus and Foitzik, 2004).

Mathematical modelling may be employed to construct and test a theory of how the cyclic transformation activity of the

Table 1
The population dynamics of distinct cell populations in the hair follicle.

Population		Anagen	Catagen	Telogen	References
SC	**No. of cells**	100–200	100–200	100–200	Waghmare et al. (2008); Zhang et al. (2010); Hsu et al. (2011)
	Proliferation	++ Early anagen. Slows by late anagen. 2–5 divisions in one hair cycle.	–	–	Wilson et al. (1994); Ito et al. (2004); Waghmare et al. (2008); Zhang et al. (2009); Hsu et al. (2011)
	Differentiation	+++ Stem cell niche/germ transition zone. To TACs and MKs	–	–	Lavker et al. (2003); Zhang et al. (2009); Hsu et al. (2011)
	Apoptosis	–	–	–	Ito et al. (2004); Hsu et al. (2011)
	Migration	To hair germ & basal layer ORS (may already be TACs)	Lateral migration in newly generated club hair	Bulge cells leave the niche	Lavker et al. (2003); Zhang et al. (2009); Zhang et al. (2010); Hsu et al. (2011)
MK	**No. of cells**	100 s	0	20–40 cells	Ito et al. (2004); Zhang et al. (2009)
	Proliferation	++++	–	–	
	Differentiation	++++ Into IRS and HS	–	–	
	Apoptosis	–	+++++	–	Lindner et al. (1997); Matsuo et al. (1998)
	Migration	–	–	–	Taylor et al. (2000)
HS	**No. of cells**	Proportional to no. of MKs. Fine distal tip, thicker mid-region, narrow proximal club	Ceases in early and mid-catagen	0	Ibrahim and Wright (1982); Tobin et al. (2003)
	Proliferation	–	–	–	
	Differentiation	+++	–	–	
	Apoptosis	–	Mid & late catagen	–	Lindner et al. (1997); Matsuo et al. (1998)
	Migration	–	–	–	
DP	**No. of cells**	Double no. in telogen. Ratio DP: MKs determines hair width	–	½ anagen	Ibrahim and Wright (1982); Tobin et al. (2003)
	Proliferation	++++ Greatest anagen IV. Rare at anagen VI	–	–	Tobin et al. (2003)
	Differentiation	–	–	–	
	Apoptosis	–	–	–	Lindner et al. (1997); Matsuo et al. (1998); Soma et al. (1998)
	Migration	+++ Into DP from CTS. In anagen VI cells migrate from DP to CTS	Early catagen: (~50% migrate to CTS)	–	

The number of cells in each population may be affected by; proliferation, differentiation, apoptosis and migration and these events are marked as present abundantly (++++) or not present (–) in line with hair cycle stages anagen, catagen and telogen. SC—stem cell, DP—dermal papilla, MK—matrix keratinocytes, CTS—connective tissue sheath, TAC—transient amplifying cell, ORS—outer root sheath, IRS—inner root sheath.

human HF originates and is controlled. Unlike other biological cycles, such as the cell cycle and the circadian rhythm, the hair cycle is comparatively unchartered territory in the mathematical modelling arena. However, a small number of mathematical models concerned with hair growth, cycling, or the synchronisation of cycling between larger HF collectives (hair waves) have been proposed (Nagorcka and Mooney, 1982; Halloy et al., 2000, 2002; Kolinko and Littler, 2000; Golichenkova and Doronin, 2008; Plikus et al., 2011).

Nagorcka and Mooney mathematically modelled the differentiation of wool and mammalian hair shaft during anagen, but did not address the cyclical processing of the human HF (Nagorcka and Mooney, 1982). Similarly, mouse hair shaft growth was modelled with respect to theoretical proliferative activity of matrix keratinocytes (MKs) (Golichenkova and Doronin, 2008). A cellular automaton model has been adopted to both simulate and predict the dynamics of populations of human (Halloy et al., 2000, 2002) and mammalian HFs (stem cell activation) (Plikus et al., 2011). A statistical model of human hair cycle laser treatment was concerned with predicting optimal timing for laser hair removal (Kolinko and Littler, 2000).

The existing models either concentrate solely on hair growth (i.e. hair shaft formation) or relate primarily to highly synchronised hair wave pattern formation in rodents. Although it has been shown that the human HF relies most heavily on its intrinsic processes to cycle (Plikus et al., 2011), none of the existing models explicitly address the intrinsic processes within the human HF that may explain the fundamental nature of the hair cycle rhythm. However, knowledge of important activators and inhibitors of the hair cycle are being elucidated in rodents (Plikus et al., 2011; Plikus, 2012). As a consequence, a persuasive mechanistic theory of how the human hair cycle is induced and maintained is still missing.

In the current contribution, we aim to outline a dynamical systems theory of the human hair cycle using mathematical modelling. We do so from the viewpoint that a dynamical instability underlies human HF cycling.

1.2. Model design

No molecules, genes or individual cells have as yet been identified as being the central "pacemaker(s)" for the hair cycle rhythm. Here, we propose an abstraction from the consideration of the vast number of specific genes, molecules, interlinking pathways and cell–cell interactions that may potentially be involved in HF cycling. We begin by detailing basic criteria that a plausible hair cycle theory should meet and then define the key dynamic features that characterise the hair cycle. This ultimately leads us to a simple but prototypic mathematical model of human HF cycling.

1.3. Essential features of a good human hair cycle theory

A satisfactory theory of the human HF cycle should be able to explain, firstly, the autonomy of the cycle. It is particularly apparent that in the human HF the "oscillator system" governing the hair cycle rhythm is located in the HF itself (Paus and Foitzik, 2004). This is supported, for example, by the maintenance of location specific HF cycling following hair transplantation surgery (Unger, 2005). A second key feature of a hair cycle theory should explain its unique rhythmicity, i.e. a long anagen phase, extremely rapid catagen stage and relatively short telogen phase. Thirdly, the central role of the HF mesenchyme (dermal papilla (DP) and proximal connective tissue sheath (CTS)) in hair cycle control must be incorporated and explained (Paus et al., 1999; Paus and Foitzik, 2004; Tobin et al., 2003). Another important aspect that

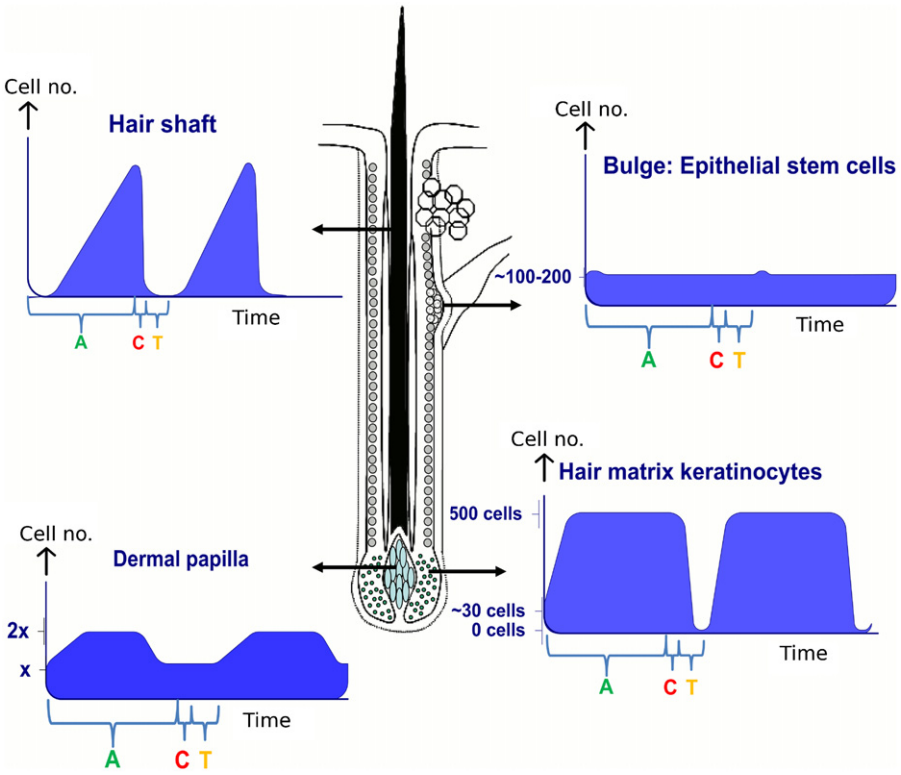

Fig. 2. Dynamic profiles of cell populations in the hair follicle. Each cell population exhibits a unique dynamic profile in line with stages of the hair cycle. Anagen (A), catagen (C) and telogen (T). The central illustration shows an anagen hair follicle. Dynamic profiles for several core hair follicle cell populations are estimates obtained from the available evidence. The schemas depict the size of each population during each cycle stage; A, C and T. This investigation into the hair cycle on the population level summaries the behaviour from a compartmentalised viewpoint. In this model, we focus on the hair matrix keratinocytes (which at numbers close to zero also captures hair germ cells in this compartment). The matrix keratinocytes population is able to capture, in the simplest form, the core events of remodelling, regression and rest during the hair cycle. In addition, the matrix keratinocytes directly supply hair shaft cells (trichocytes). This figure also demonstrates the two compartments, namely matrix keratinocytes (compartment 1) and dermal papilla (compartment 2), on which the model is constructed.

the theory should address in human hair cycling is the diverse periodicity seen in vivo between different HFs, for example how HFs located in anatomically different sites may come to vary (Courtois et al., 1994). Lastly, a satisfactory theory of the hair cycle should address or be able to generate hypotheses as to how HFs might respond to specific treatment and how known hair disorders may arise from disturbances in the normal cycling activity of healthy human HFs.

1.4. Identifying the key processes and dynamical changes in the hair cycle

The HF is a highly dynamic mini-organ in which multiple distinct cell populations that originate from mesoderm or (neuro) ectoderm intimately interact in a precisely coordinated fashion in order to temporarily and rhythmically generate a (usually pigmented) hair shaft (Fig. 1). The HF is predominantly constituted by epithelial cells whose activities are controlled by specialised mesenchymal cells, i.e. inductive fibroblasts of the DP and the CTS. Jointly, these epithelial and mesenchymal cell populations control the activity of neural crest-derived, specialised melanocytes of the HF pigmentary unit (HFPU) (Schneider et al., 2009; Tobin, 2011). All three interacting cell populations arise from and are replenished by epithelial (or melanocyte) stem cells that are mainly located in the so-called bulge region of the outer root sheath or the secondary hair germ that forms between the DP and the club hair during the regression of anagen HFs, or from stem cells located in the HF mesenchyme (Fig. 1).

Dramatic structural changes, inextricably linked to a dynamic redistribution of cell populations, occur in the HF as it processes cyclically through the three stages of the hair cycle after morphogenesis (catagen→telogen→anagen→catagen) (Paus and Foitzik, 2004). In order to establish the core events that may be responsible for the hair cycle rhythm, the necessary cell populations, processes and interactions characterising the major cyclical HF transformations must be defined. A summary of these features during each hair cycle phase is provided in Table 1 and Fig. 2. Where available, estimates of population numbers are given. The bulge region and the secondary hair germ of the HF houses epithelial stem cells. Approximately 100–200 stem cells are located in the bulge of mouse pelage HFs (see Table 1; note that at present there are no reliable data available for the number of epithelial stem cells in the human bulge). Proliferation of these epithelial stem cells occurs during late telogen and early anagen probably following activation by DP fibroblasts (Fig. 2) (Ito et al., 2004; Waghmare et al., 2008; Greco et al., 2009; Zhang et al., 2010). The progeny of bulge epithelial stem cells (transient amplifying cells (TACs)) proliferate to create the ORS (outer root sheath) and can regenerate the entire HF epithelium (Levy et al., 2005, Zhang et al., 2009). Possibly, the inner root sheath (IRS) and hair matrix arise from an epithelial progenitor cell population located in the secondary hair germ, which originated from bulge stem cells (Panteleyev et al., 2001; Ito et al., 2004).

It is not clear at present whether the processes of proliferation and migration cause the number of stem cells to periodically increase during the hair cycle or whether this activity only leads to the production of more committed, semi-differentiated cells

(TACs), without changes in stem cell number (Wilson et al., 1994; Lavker et al., 2003; Ito et al., 2004; Zhang et al., 2009) (see Fig. 2 and Table 1). Although there is evidence of apoptosis in the murine HF bulge during catagen (Lindner et al., 1997), apoptosis is thought to play a negligible role in the bulge stem cell niche, as these cells are spared from extensive apoptosis that characterises catagen in the proximal HF epithelium. This preserves a vital cell pool that remains permanently available for HF regeneration (if epithelial HF stem cells get depleted in pathological conditions, this results in scarring alopecia) (Harries and Paus, 2010). Therefore, an important tenet for the design of the hair cycle model is the assumption that the stem cell population within its niche remains largely constant and serves as a permanent pool for hair MKs and other epithelial compartments of the HF (Fig. 2).

MKs arise from the differentiation of TACs, which themselves arise from epithelial stem cells (Fig. 2). During anagen, MKs undergo rapid proliferation and then terminally differentiate into various epithelial lineages that form the hair shaft and the IRS. The ORS appears to be largely generated by the immediate progeny of the TACs that have arisen from HF epithelial stem cells in the bulge (Cotsarelis, 2006; Panteleyev et al., 2001; Ito et al., 2004). When MK cells proliferate they do so to replace those that have already undergone terminal differentiation into the hair shaft and IRS (Fig. 2). Thus, another important tenet of our hair cycle theory is that the population size of MKs determines the size of cell population available for hair shaft and IRS production.

In adult human scalp skin, hair shaft production follows an approximately linear growth pattern in vivo, with the hair shaft thinning at the end of anagen (Ibrahim and Wright, 1982). Even microdissected and amputated hair bulbs of terminal human scalp HFs in anagen VI demonstrate the same hair shaft production speed as the living human scalp (Philpott et al., 1990). In Fig. 3 we demonstrate the hair shaft elongation rate of anagen scalp HFs isolated from 18 different human individuals, whereby the linearity of hair shaft production is shown. Therefore, our mathematical model proposed below aims to produce a similar, approximately linear, human hair growth pattern (Figs. 2 and 3).

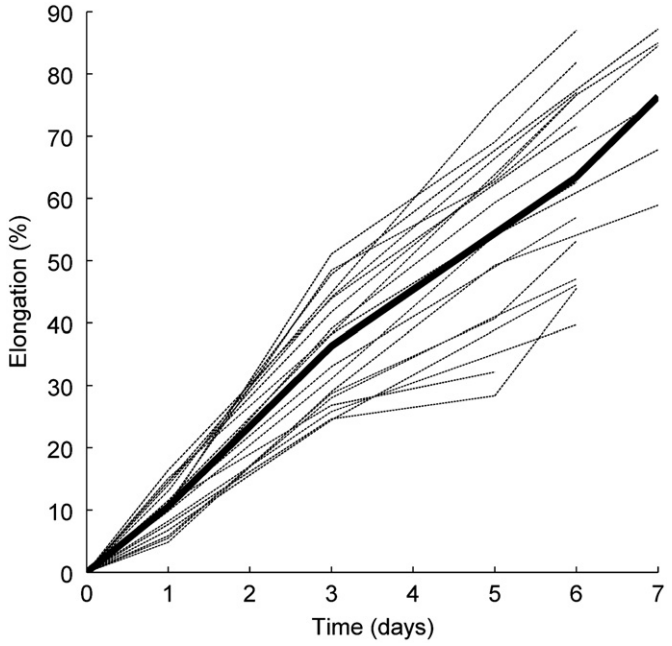

Fig. 3. Elongation of human hair follicles in organ culture. Human hair follicle elongation data obtained from 18 patients (each patient is shown as the light grey lines) and the average percent elongation of the 18 patients is shown by the thick black line.

However, while hair shaft formation is linear, HF cycling is not. Each hair cycle phase is of divergent length (for example, catagen lasts weeks compared to anagen having a duration of years in human terminal scalp HFs) (Paus and Foitzik, 2004). In order to understand the process of each hair cycle stage, we now take a closer look at catagen, the regressive phase of the hair cycle.

Catagen heralds the complete elimination of MK cells via apoptosis (Lindner et al., 1997). The population remains at or near zero during telogen until the onset of the next anagen phase. When MKs undergo apoptosis in catagen, the supply of cells to the hair shaft is interrupted and hair production ceases. Very early during the anagen–catagen transformation, intrafollicular melanogenesis and all melanosome-based transfer of melanin from HFPU melanocytes into future hair shaft keratinocytes (trichocytes) is abruptly terminated (Tobin et al., 1998; Slominski et al., 2005; Tobin, 2011). As a result, the old hair shaft from the preceding anagen phase is transformed into a so-called "club hair", whose proximal end is non-pigmented. This club hair is subsequently shed during exogen or is pushed out by the new hair shaft that is generated in the next anagen phase (Higgins et al., 2009).

The dynamics of the MK cell population encompasses all key phenomenological cyclical events of (i) hair production during anagen, (ii) cessation of hair production during catagen and telogen, and (iii) production of a new hair with each anagen phase. MK apoptosis during catagen results in involution of the lower two thirds of the HF whereas MK proliferation during anagen represents a key event of cyclical HF regeneration. Since MKs produce hair via anagen-coupled terminal differentiation, the dynamics of the MK population have a crucial role in abnormalities such as hair loss, which are best understood to be pathologies of HF cycling dynamics (Paus et al., 1999; Paus and Foitzik, 2004; Paus, 2006). Therefore, the MK population shows the most overt and dramatic changes of cell populations within the HF with proliferation, differentiation and apoptosis identified as key processes dictating these changes (Fig. 2 and Table 1). In addition, MKs are extremely sensitive to damage (e.g. by drugs, reactive oxygen species, radiation, inflammatory mediators, metabolic and hormonal abnormalities) and thus play a crucial role in multiple different hair loss disorders (Paus, 2006; Bodó et al., 2010). Therefore, we identify MKs as the optimal cell population to focus on when developing a simple mathematical model of HF cycling operating at the level of tissue dynamics.

The CTS and the DP constitute the HF mesenchyme, without which proper HF morphogenesis and cycling are impossible. Indeed, inductive signals from CTS and DP fibroblasts are essential for the epithelial–mesenchymal crosstalk that drives HF cycling (Botchkarev and Kishimoto, 2003; Yang and Cotsarelis, 2010). The DP sits in the centre of the hair bulb epithelium and is directly connected to the CTS by the dermal stalk, with MKs enveloping the DP from all sides during anagen (Figs. 1 and 2). Inductive fibroblasts of the HF mesenchyme utilise the stalk of the DP as a trafficking conduit through which cells immigrate into the DP during early anagen and emigrate during catagen (Tobin et al., 2003; Kloepper et al., 2010).

A special, dynamically remodelled basement membrane separates MK and DP cells and is needed for proper epithelial–mesenchymal communication in the HF (Link et al., 1990). The unique nature of the bidirectional communication between these two cell populations is evident from the fact that this membrane becomes fenestrated during anagen and that DP fibroblasts have cell processes that protrude into the innermost layer of the hair matrix (Nutbrown and Randall, 1995; Matsuzaki and Yoshizato, 1998; Stenn and Paus, 2001). Without fully functional bidirectional communication between MKs and DP cells HF cycling becomes grossly disturbed and eventually ceases altogether. If the disturbance persists, HFs become dystrophic and eventually disappear (Panteleyev et al., 1999; Ohyama et al., 2010).

The dynamics of the DP are mainly determined by bidirectional, hair cycle-dependent fibroblast migration between the DP and the proximal CTS (Fig. 2 and Table 1) (Tobin et al., 2003). Under physiological conditions, there is extremely little, if any, apoptosis in the DP during the hair cycle, even in catagen and even under conditions that induce massive MK apoptosis (such as chemotherapy (Lindner et al., 1997)). Also, fibroblast proliferation within the DP is a rare event and may essentially be limited to a narrow window during anagen development (Tobin et al., 2003; Paus and Foitzik, 2004). Therefore, as MK-DP cell interactions are undoubtedly crucial for normal HF cycling, signals emanating between the two compartments need to be incorporated in the model. However, for simplicity's sake, DP cell numbers shall not be explicitly modelled.

To summarise the basic concepts that underlie the subsequently proposed model of HF cycling, the hair cycle is underpinned by dynamic changes at the level of defined cell populations. Among these, MKs are a crucial cell population on whose analysis a theory of HF cycling can be based. This is since MK dynamics most perfectly reflect all key phenomena that underlie HF cycling, i.e. rhythmic changes in (i) proliferation, (ii) apoptosis, and (iii) differentiation (Fig. 2 and Table 1). In addition, since communication between epithelial MK and the mesenchymal HF is essential for hair cycling, our attempt of a dynamical theory of human HF cycling will be based on a mechanistic mathematical description of MK cell numbers (changes in which result from MK proliferation, terminal differentiation or apoptosis) with communication provided between the MKs and DP. By highlighting the behaviour of selected HF cell populations and understanding the processes that govern the changes in cell numbers, we are able to specify a set of fundamental observations that should be captured in an adequate model for hair cycle dynamics. The most salient of these features is the asymmetric duration of each phase of the hair cycle. We now proceed to a mathematical formulation of human HF cycling.

2. A prototypic human hair cycle model

2.1. Model formulation

On the basis of the features elaborated above (Fig. 2 and Table 1) we formulate the following model for human HF cycling. The model focuses on the dynamics of MK cells with respect to the population level processes of proliferation, apoptosis and differentiation. A schematic overview of the model is provided in Fig. 4.

In general, the dynamics of MK cells, x, under these processes, can be captured mathematically as follows:

$$\frac{dx}{dt} = f(x) - g(x) + (a - bx) \tag{1}$$

The two functions, f and g, represent proliferation and apoptosis, respectively, and are in general nonlinear. The assumption of nonlinearity here allows us to proceed to formulate the hair cycle oscillation in terms of ordinary differential equations. In the following results we highlight the important emergent properties that follow from these assumptions, while we must leave the thorough experimental and theoretical investigation of the exact nature of apoptosis and proliferation controls in the HF to future studies. We note that both are assumed to depend on the state of the system, i.e. the size of the MK population. Parameter a represents a constant input to the population from stem cells and the term bx encompasses all processes leading to a decrease in the number of MKs apart from apoptosis, including differentiation.

We assume saturation in growth, which is modelled with a saturation function, e.g. $p_1 x^n/(p_2^n + x^n)$. This assumption is justified as growth of MKs is likely to saturate depending upon factors such as the supply of nutrients (which are not modelled explicitly here). The simplest case is when $n = 1$ which leads to a hyperbolic function. The apoptotic function, g, follows a similar form, however we also include the possibility for feedforward inhibition via

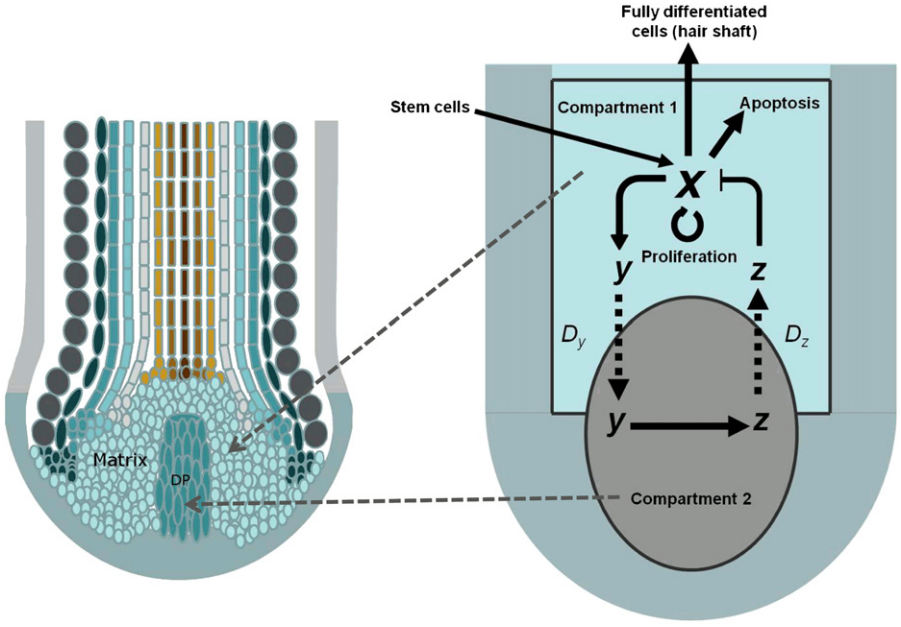

Fig. 4. Schema of the two compartment model. x denotes the matrix keratinocyte population in compartment 1 (epithelial hair follicle). Processes affecting the size of x are a constant stem cell input, a proliferation process, an apoptotic process and a constant linear output denoting the differentiation of matrix keratinocytes into the other cell types, i.e. layers of the inner root sheath and hair shaft. Compartment 2 is the dermal papilla. Bidirectional communication between compartments 1 and 2 is set up by the production of a variable y that diffuses into compartment 2 causing the production of z. z diffuses back into compartment 1 where it affects proliferation and apoptotic processes for x.

the exponent, k:

$$\frac{dx}{dt} = \frac{p_1 x}{(p_2+x)} - \frac{p_4 x}{{p_5}^k + x^k} + (a - bx) \quad (2)$$

Within this framework, we introduce communication between the MKs and the DP. It is assumed that feedback with the DP affects either proliferation or apoptosis of MKs, for example via papilla morphogens or endogenous inhibitors (Paus et al., 1999; Stenn and Paus, 2001; Botchkarev and Kishimoto, 2003). These processes enter as additional terms in f and g, dependent upon a new variable, z. Here, we consider negative feedback only, introducing terms for feedback inhibition of the proliferative term and feedback activation of the apoptotic term. The specific forms of feedback that allow for bistable and oscillatory solutions are chosen according to the general analysis of reaction networks (Tyson, 2002). This is applicable because the population models follow a structure similar to reaction kinetic models. In future experiments the functional form of degradation and the effect of feedback inhibition can be further examined. In the theory we present, these experiments would require isolation of the morphogen, z, and attenuation of its function in order to gauge its effects and to observe the form of decay of x in the absence of z. The assumptions above lead to the following form:

$$\frac{dx}{dt} = \frac{p_1 x}{(p_2+x)(p_3+C_{prol}z_1)} - \frac{(p_4+C_{apop}z_1)x}{{p_5}^k + x^k} + a - bx \quad (3)$$

Here, constants C_{prol} and C_{apop} regulate the strength of feedback of z on the population equation for x. In the present contribution we focus on the role of proliferation control (governed by parameter C_{prol}). We briefly explore the effect of apoptotic control (governed by parameter C_{apop}) on the cycling behaviour but leave a detailed investigation of this term for future research. The index in variable z refers to the two-compartment version described below.

Since communication between the hair matrix and DP are key to the hair cycle these spatial considerations are taken into account in the model (Fig. 4). We start with the simplest formulation of communication between two compartments, which is assumed to be mediated by signalling molecules. Specifically, we use the following set of differential equations:

Compartment 1

$$\frac{dx}{dt} = \frac{p_1 x}{(p_2+x)(p_3+C_{prol}z_1)} - \frac{(p_4+C_{apop}z_1)x}{{p_5}^k + x^k} + a - bx$$

$$\frac{dy_1}{dt} = c_1 x + D_y(y_2 - 2y_1)$$

$$\frac{dz_1}{dt} = D_z(z_2 - 2z_1) \quad (4)$$

Compartment 2

$$\frac{dy_2}{dt} = D_y(y_1 - 2y_2)$$

$$\frac{dz_2}{dt} = c_2 y_2 + D_z(z_1 - 2z_2)$$

It is assumed here that the MK population (compartment 1) produces a signalling molecule y (at rate c_1) which produces no further direct effect on the population dynamics. However, it diffuses away from the compartment and can thereby either disappear altogether (being degraded or having diffused into compartments where it exerts no significant hair cycle effect) or it can diffuse into compartment 2 (the DP) where it induces the production (or activation) of a regulatory molecule z at rate c_2. This regulator, in turn, exerts no effect in the DP but can diffuse into either the surroundings or into compartment 1. In compartment 1, control of the keratinocyte population is then performed by the regulator via proliferation inhibition or apoptosis activation as in the model Eq. (4). The diffusion processes take place at two different rates (D_y and D_z) which are the permeation constants in the present model. They would turn into formal diffusion constants in a space-continuous reaction-diffusion model. The factors of 2 in the differences modulated by D_y and D_z indicate that the diffusion between compartments is not mass conserved, i.e. that there is leakage into the surrounding environment. In the equation for dz_1/dt, for example, which represents the amount of z in compartment 1, we include a positive term $D_z z_2$ to model incoming z from compartment 2. In addition there are 2 negative terms, $-D_z z_1$, which represent diffusion of z into compartment 1 and diffusion of z into the surround, respectively. As a simplifying assumption, the diffusion between compartments and into the surround is assumed equal. For all of these processes we use first order differential equations as used, for example, in models of (bio)chemical reactions.

2.2. Addition of hair shaft growth to the model

Hair shaft production is the most distinctive output of the HF. It can be considered a marker for healthy HF function and normal HF cycling dynamics. Therefore, hair shaft production was added to the model via an additional variable. A growth rate proportional to the MK population, $dh/dt = x$, is assumed in accordance with the relationship between the MK cell population size and hair shaft production as discussed in Section 1.4 (Figs. 2 and 3). In order to simulate the termination of hair growth during telogen (relative quiescence) we introduce an algorithm which "wraps" the hair length back to zero during this stage. This is achieved by locating the plateau as a period of small increase in growth and applying a threshold to the derivative of the hair growth variable h. During time periods below this threshold, the hair length is reset to zero, with hair beginning to grow again once the threshold is traversed.

3. Results

3.1. The unperturbed model

In this section we analyse the model Eq. (4) in terms of its key nonlinear components, the power k in the apoptotic term and the influence of feedback in the proliferation term. Using the hair growth variable h as output, we then demonstrate the capability of the model to reproduce key features of the human hair cycle. Since we are ultimately interested in applying the model to hair pathology and its treatment, we also investigate some features of abnormal (non-oscillatory) dynamical behaviour. In the following section we report some results on the model's response to external stimuli.

3.1.1. Steady state for $C_{prol}=0$ and $k=1$

Fig. 5 shows bifurcation diagrams scanning one of the system parameters, namely, the growth rate p_1, for different values of C_{prol} and k. All other parameters are fixed to the values displayed in Table 2 and are non-dimensional along with the formulation of the model. The simplest case is $C_{prol}=0$ and $k=1$, i.e. there is no feedback loop in the model and the apoptotic rate is modelled as a hyperbolic function as is the proliferation rate. This reduces the model to a one-dimensional system that can only have steady state solutions. Fig. 5a shows the corresponding bifurcation diagram. At $p_1 \approx 0.04$ there is a transcritical bifurcation leading to an abrupt change of slope in the otherwise linear dependence of the steady state value on p_1. Such behaviour predicts that the

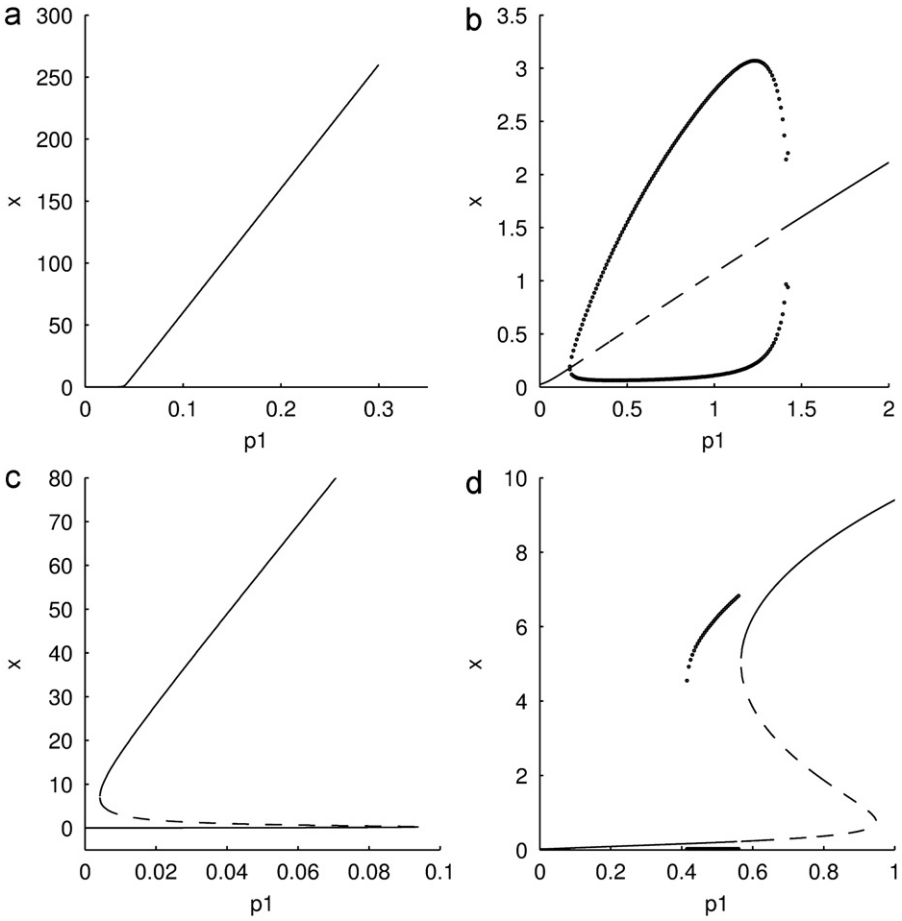

Fig. 5. Bifurcation diagrams of the matrix keratinocyte population, x, in Eq. (4) as a function of growth constant p_1 for different values of k and C_{prol}. (a) $k=1$, $C_{prol}=0$, and $p_5=0.1$; (b) $k=1$, $C_{prol}=1$ and $p_5=0.1$. (c) $k=2$, $C_{prol}=0$, and $p_5=\sqrt{0.1}$. (d) $k=2$, $C_{prol}=1$, and $p_5=\sqrt{0.1}$. Feedback inhibition is required to produce cycling behaviour for $C_{prol}=1$ in (b). There is bistability for $k=2$ in (c). In (d) there is combined bistability and oscillations when $k=2$, $C_{prol}=1$. Other parameters as in Table 2.

Table 2
Default parameter values used in the hair cycle model.

Parameter	Value	Parameter	Value
a	0.1	C_{prol}	1
b	0.01	C_{apop}	0
p_1	0.48	C_1	1
p_2	0.1	C_2	1
p_3	0.1	D_y	0.5
p_4	0.5	D_z	0.1
p_5	0.32		

Alterations to the parameter values in the study are listed in the figure legends or in the text in the relevant sections.

dependence of an observed temporally stable keratinocyte population shows different rates of change as a function of the population growth rate. It cannot, however, account for autonomous cycling of the population nor does it allow for an interpretation of discrete growth states (anagen and telogen).

3.1.2. *Hopf oscillations for $C_{prol}=1$ and $k=1$*

When $C_{prol}=1$, the keratinocyte population is additionally influenced by the regulatory factor z, implying that the model is now composed of 5 dependent variables. Therefore we now have a control loop that results in feedback inhibition because an increase in the concentration of z results in a decrease of the growth rate of the keratinocyte population. Feedback inhibition is implemented in our model via a two-species mechanism involving communication between the two compartments (Fig. 4). Such feedback is necessary and in our case sufficient to produce cyclical behaviour (Fig. 5). The oscillatory behaviour is seen for a wide range of parameter p_1. Its amplitude depends strongly and nonlinearly on the value chosen and shrinks to zero as either bifurcation point is approached. A time series of the oscillation is shown in Fig. 6a (grey) and a phase space representation of the underlying limit cycle is shown in Fig. 6b (grey). Mathematically, the oscillations result from a dynamical instability of a steady state. The specific instability in Eq. (4) is a supercritical Hopf bifurcation with the real part of a pair of complex eigenvalues passing from negative to positive. This happens twice and therefore the oscillatory region is bounded by stable fixed point behaviour. All mathematical terms relating to this feedback loop are linear with the exception of the control of the MK population by species z, originating in the DP. Therefore, the nonlinearity that causes self-organising instabilities in our model resides in the equation for the keratinocyte population.

This form of the equation with $C_{prol}=1$ and $k=0$ is therefore a variant of the kinetic feedback inhibition oscillator proposed by Goodwin (1963). Here, the delay in the feedback to the keratinocyte population is in part due to transport processes that mediate the feedback. A fast oscillating keratinocyte population is produced by these conditions and thus, feedback is demonstrated to be important to gain cyclical behaviour in the human hair cycle according to this model.

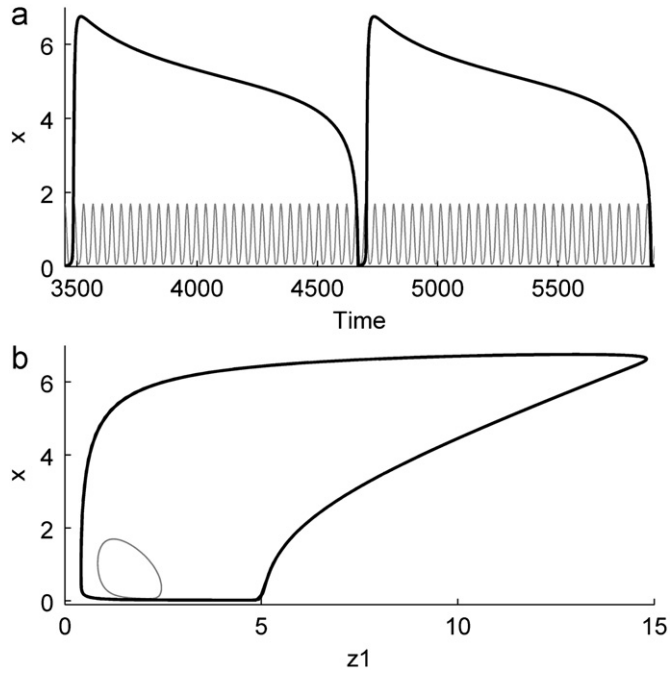

Fig. 6. Hair cycle time series and phase space for $C_{prol}=1$ and $C_{apop}=0$. (a) Time series of matrix keratinocytes x for $k=2$ and $p_5=0.32$ (black line) and $k=1$ and $p_5=0.1$ (grey line). (b) Matrix keratinocyte population versus inhibitor z_1 for $k=2$ and $p_5=0.32$ (black line) and $k=1$ and $p_5=0.1$ (grey line). Other parameters as in Table 2.

3.1.3. Bistability for $C_{prol}=0$ and $k=2$

If forward inhibition of the apoptotic process is included instead of feedback control (i.e. $k=2$) the dynamics of the keratinocyte population remains independent of other processes but shows a new type of dynamical phenomenon. Fig. 5c shows that this situation generates a region of bistability (compare with Fig. 5a). Two fixed point solutions (represented by black lines) can be observed for a finite range of parameter p_1. This is due to the appearance of three (real) steady state solutions in the fixed point equation for x ($dx/dt=0$). In such a situation, when parameter p_1 is varied across the borders of the region of bistability, the system can be induced to change from one steady state to the other (e.g. switching from a near-zero to large value when p_1 is increased above a value of 0.09, see Fig. 5c). We therefore explore a bistable switch as a possible mechanism for HF dynamics. The lower steady state would represent "telogen" and the upper steady state "anagen". In our model one possible realisation of switching would be that random fluctuations of the keratinocyte population result in (self-organised) switching between the states. Mathematically, the two stable states are separated by an unstable state which corresponds to a critical population size that lies between the no growth and the growth state (Fig. 5c). This critical population size presents a decision point. If a random fluctuation in the no growth state exceeds the critical size, the population will continue to grow until it reaches the growth state, where it will remain. Switching back will occur when a random fluctuation of the population in the growth state reaches a value that lies below the critical state. The population will then keep shrinking until it falls to the "no growth" state. In contrast, if a perturbation leads to a change close to the critical size but not quite reaching it, the population reverts to the original state.

Adding a noise term to the model Eq. (4) with $k=2$ and $C_{prol}=C_{apop}=0$, the amplitude of the noise can be adjusted such that it leads to random variation about a given steady state. When preparing the model in the bistable region near the critical parameter value where the no growth state disappears ($p_1\approx 0.09$), we can adjust the model in the presence of noise perturbations such that the mean duration in anagen is much longer than the duration in telogen as is the case in human hair cycling. However, careful preparation of the parameters of the model is required to reproduce these characteristics. As in the case of Fig. 5a, the exclusively steady state solutions found do not allow for the explanation of an organised cyclical process.

3.1.4. Relaxation oscillations for $C_{prol}=1$ and $k=2$

In light of the above considerations, where neither the supercritical Hopf oscillations nor the bistability alone may fully account for the dynamics of the HF, we further explore the impact of the two parameters using a combination of both. In this case, there is a feedback control of the keratinocyte population by variable z and forward inhibition by the population itself, i.e. $C_{prol}=1$ and $k=2$. Fig. 5d shows the corresponding bifurcation diagram where a region of bistability and a limit cycle region are indicated by a dotted bar. In this case, the forward inhibition again generates a region of bistability. However, compared to the situation with $C_{prol}=0$ (bistability of two fixed points), the bistability is between a near-zero fixed point and a limit cycle (compare Fig. 5c and d). The bistable region starts with a fold of limit cycles bifurcation at $p_1\approx 0.415$ and ends with a subcritical Hopf bifurcation at $p_1\approx 0.51$.

The limit cycle is generated in the aforementioned fold of limit cycle bifurcation at $p_1\approx 0.415$ and vanishes with a saddle-node on limit cycle bifurcation at $p_1\approx 0.56$. In comparison with the situation in Fig. 5b (no forward inhibition) the oscillations start and vanish abruptly, i.e. with finite amplitude at the bifurcation point. The variation of amplitude in this region is much smaller than in the situation with $k=1$. Further differences between the dynamics of the limit cycles in the cases of Fig. 5b and d are shown in Fig. 6 where time series (Fig. 6a) and phase space portraits (Fig. 6b) are plotted for $k=1$ and $k=2$. The Hopf cycle ($k=1$) has a small amplitude, high frequency, and a comparatively harmonic waveform. The cycle with $k=2$, in contrast, has a large amplitude, low frequency, and strongly asymmetric waveform. Notable generic features of this latter, non-harmonic limit cycle are:

(i) Two plateau-like phases where the change of state is comparatively slow. One is near zero and the other has an amplitude between 4 and 7 approximately. Both phases can be related to the two respective fixed points in the bistable situation with $C_{prol}=0$ and $k=2$ as shown in Fig. 5c.
(ii) Comparatively fast transitions between the two plateau-like states.
(iii) Notably, the durations of the two plateau-like states differ strongly with a long upper state and a short lower state being a consistent finding in the present model.

Taken together, features (i) and (ii) define a type of dynamics classified as relaxation oscillations. The notable properties above directly relate to the dynamics of the HF (Fig. 2—matrix keratinocytes). The long upper steady state is interpreted as anagen, the short lower state as telogen and the rapid transition from growth to rest as catagen. Asymmetry in phase durations in each stage is representative of the durations of anagen (long), catagen (very short) and telogen (intermediate, but relatively short compared to anagen). The strong asymmetry in the cycle is explained by the vicinity of a saddle-node on limit cycle bifurcation which causes slowing down of the anagen phase but not of telogen. Therefore, the dynamics of the HF model requires both bistability and

feedback inhibition, as achieved here with $k=2$ and $C_{prol}=1$ to approximate the key features of the HF cycle.

In this version of the hair cycle model, the oscillatory time series of the other variables (y and z) produce, in comparison, a qualitatively similar waveform to the one described for the keratinocyte population. However, at a shorter time scale there are significant phase shifts between oscillations in the two compartments and between the oscillations of the keratinocyte population and the concentration of the feedback species z_1.

So far, we have only considered feedback on the apoptotic term in Eq. (4). If the feedback loop to the keratinocyte population is instead closed in the apoptotic component ($C_{prol}=0$ and $C_{apop}=1$), this results in a similar overall result to the above formulation. Model simulations with a parameter setting of $C_{prol}=0$ and $C_{apop}=1$ equally produce relaxation oscillations with an asymmetric waveform and distinct growth and resting phases Fig. 7. The phase space structure is not identical but qualitatively similar, the only significant difference being the large amplitude in the present case (compare Figs. 6 and 7). The differences are due to the asymmetry of the proliferation and apoptosis terms with $k=2$. Model settings with both feedback controls switched on (e.g. $C_{prol}=1$, $C_{apop}=1$) also produce large amplitude, low frequency relaxation oscillations.

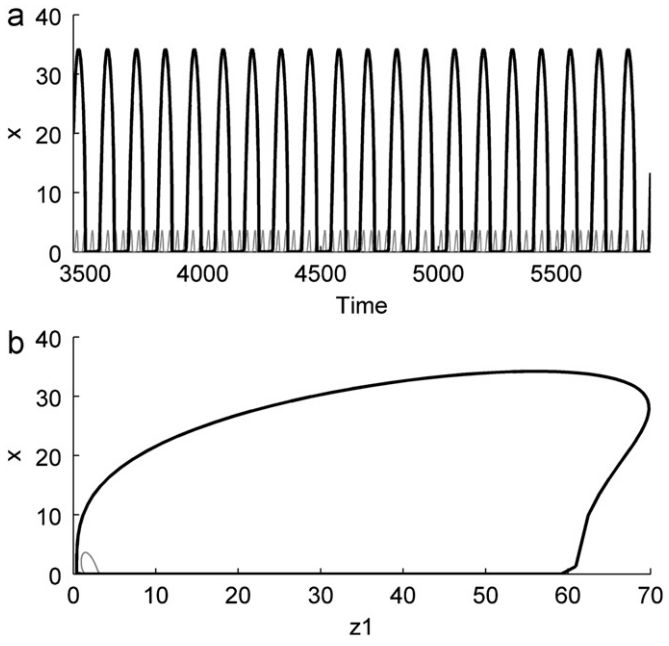

Fig. 7. Alternative hair cycle mechanism for $C_{prol}=0$ and $C_{apop}=1$. (a) Time series of matrix keratinocytes for $k=2$ and $p_5=0.32$ (black line) and $k=1$ and $p_5=0.1$ (grey line). (b) Limit cycle in phase space as in Fig. 6 for $k=2$ (black) and $k=1$ ($p_5=0.1$) (grey). Other parameters as in Table 2.

For simplicity, we only explore feedback on the proliferation term ($C_{prol}=1$, $C_{apop}=0$) in all studies below. A detailed exploration of apoptotic control must be left for an extended version of the model including greater details of the bidirectional communication exchanges between the DP and the MK compartment (Fig. 4).

In Fig. 8 we provide an exploration of the behaviour of the system with respect to changes in four further model parameters. This provides an initial investigation of the sensitivity of hair follicle oscillations in the model. The scan of parameters a and p_2 demonstrates the area of oscillations for $a \leq 0.1$ and $p_2 \leq 0.2$ (Fig. 8a). The frequency of the oscillations is smallest for large a and p_2. In this scan the fixed point coexists with the limit cycle throughout the scanned region. However, we find the basin of attraction of the fixed point to be small. The scan of parameters b and p_5 shows oscillations for $p_5 \geq 0.2$ and $b \geq 0.1$ (Fig. 8b). Here, the frequency is small for small p_5 and b. In addition, there is a limited region of bistability between the oscillatory and the non-oscillatory state (marked in red).

We finally consider hair production in the model in relation to the state of the MK population. The near zero-state of the population defines a no growth phase and the upper state defines a period of strong growth. As a passive output of the oscillatory model in Fig. 9 hair shaft growth has a saw tooth-like waveform interrupted by brief "no growth" periods (shown in Fig. 9b, middle and right panel). We verified the experimental growth pattern of isolated human HFs (total number of HFs=347) in organ culture from 18 patients. The growth pattern fits the model output with an almost linear shape (see Figs. 3 and 9). Human HF organ culture has been shown to grow at approximately the same rate as that in vivo (Philpott et al., 1990; Kwon et al., 2006) and therefore the reproduction of this supports the model as an approximation of the hair cycle and hair growth.

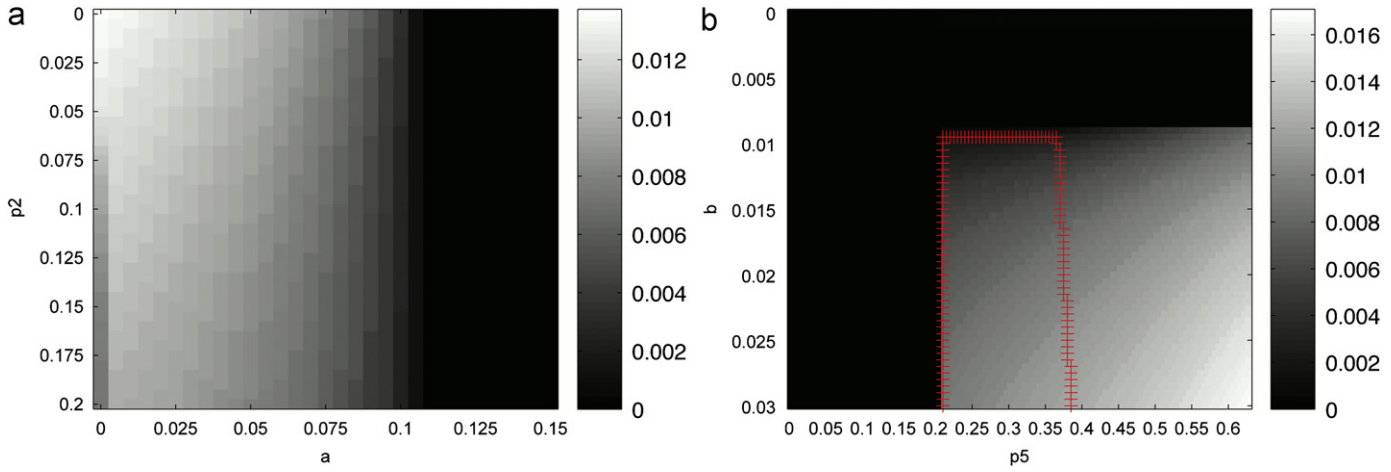

Fig. 8. Sensitivity of the model HF oscillation. Parameter scans of matrix keratinocyte dynamics: (a) parameters a and p_2; (b) parameters b and p_5. Black indicates stable fixed point; the grey scale represents the (dimensionless) frequency of oscillations as given by the scale bars. The region delineated by red crosses in (b) indicates a region of bistability between oscillations and a stable fixed point. (For interpretation of the references to color in this figure legend, the reader is referred to the web version of this article.)

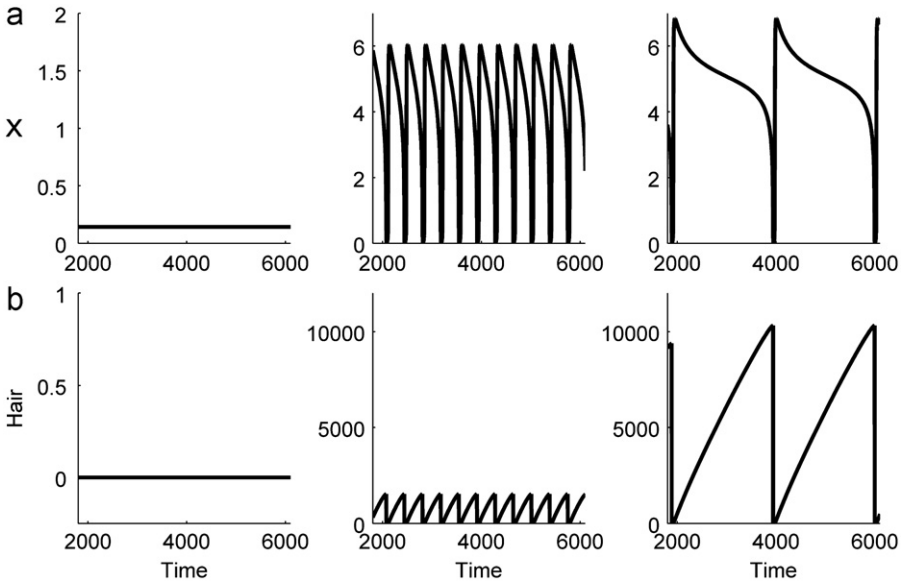

Fig. 9. Hair cycling and hair shaft growth patterns for different values of p_1. Time series of (a) matrix keratinocytes and (b) hair shaft production. Left panel: no cycling, $p_1=0.35$; middle panel: high frequency hair cycle and small hairs, $p_1=0.48$; and right panel: very low frequency cycling and long hairs, $p_1=0.56$. The transition of the hair follicle in alopecia via the process of miniaturisation may be captured in these transitions whereby the hair follicle shrinks and produces small, ineffective hair (e.g. p_1 alters from right to left here). In severe cases of alopecia no visible hair is seen which may be captured by; either short hairs that do not reach the surface (middle panel) or a transition to the no growth situation (left panel).

3.2. Perturbations of the hair cycle

We now take the oscillatory model output presented in Section 3.1 as representing healthy hair cycle dynamics and study its properties (as well as the properties of the "no growth" state) under external perturbation. The investigation here aims to realise the impact of (i) temporal variation of the environment; (ii) external pulses applied during regular growth; and (iii) pulse perturbations ("treatment") under abnormal ("no growth") conditions.

3.2.1. Variation of parameters demonstrates a range of dynamics in hair cycling that may account for both normal hair cycling and pathological states

The model predicts different hair cycling lengths depending upon the efficacies of the underlying mechanisms; i.e. different regions of parameter space. The HF does not always cycle and can be arrested in telogen for an abnormally long time period, e.g. in situations of advanced alopecia, and demonstrates transformation in size and dynamic properties depending on skin location or in the context of hair pathology (Dawber, 1997). HFs are of greatly varying size and produce different types of hair shafts of very divergent length and width, depending on the body region (Dawber, 1997). The model, as evident by the bifurcation diagram Fig. 5d, is able to reproduce variations in the hair cycle lengths depending on certain conditions in the model. In Fig. 9 we demonstrate the output of the model with different values of p_1 with respect to the number of MKs and also the dynamics of the resultant hair shaft. This could potentially explain the various HF sizes and hairs seen in vivo and additionally the potential output of no hair growth (Fig. 9, bottom left panel).

3.2.2. Pulse perturbation results in changes in normal hair cycling and pathological states

We explored the effect of a pulse perturbation in the key parameters a (stem cell supply), p_1 (proliferation rate), and p_4 (apoptosis rate). Initially the time, duration and amplitude of an individual pulse to each of these parameters was fixed. Fig. 10 shows the result of selected perturbations to the HF oscillator in the standard state (monostable relaxation oscillations). In Fig. 10a one sees a pulsed increase in parameter p_1 during telogen that leads to a subsequent prolonged anagen phase (in this case approximately a 50% increase compared to the unperturbed phase) and consequently the production of a longer hair shaft.

A similar pulse perturbation of parameter a (stem cell input) produced an increase in anagen phase duration (in this case about 90% increase compared to unperturbed phase) and hair length (Fig. 10b). Since the increase in parameter a is proportionally higher than that of p_1 (i.e. 90% increase in parameter value), the effect of this increase is larger and produces a much longer hair shaft.

The administration of a pulse to parameter p_4 within the resting phase produced a prolonged resting phase and also led to greater duration and amplitude of the subsequent growth phase (Fig. 10c). In contrast, when a pulse in the same parameter was administered during the growth (anagen) phase, anagen duration and the resultant hair length were shortened (Fig. 10d). Therefore, a phase dependent effect is seen here. Regular maintenance of the change would require regular administrations of pulse perturbations or "treatment" at the correct phase of the hair cycle.

3.2.3. Switching in bistability and excitability as methods of transition from "no hair growth" to the cycling mode

We now explore the model's features outside the parameter range where the relaxation oscillator is the only solution. The parameters are chosen in the region of bistability where both relaxation oscillations and a lower "no growth" steady state exist. In this setting we explore the possibility to perturb the system with a pulse to switch behaviour from fixed point to the oscillatory state, i.e. to induce oscillations without permanent changes in any parameter.

The time series (Fig. 11a) demonstrates a switch from the lower steady state into the oscillatory regime. Oscillations, and hair growth commence as soon as the perturbation has ended. Importantly, as the oscillatory regime is stable, the cycling continues indefinitely in the model. We tested perturbations in

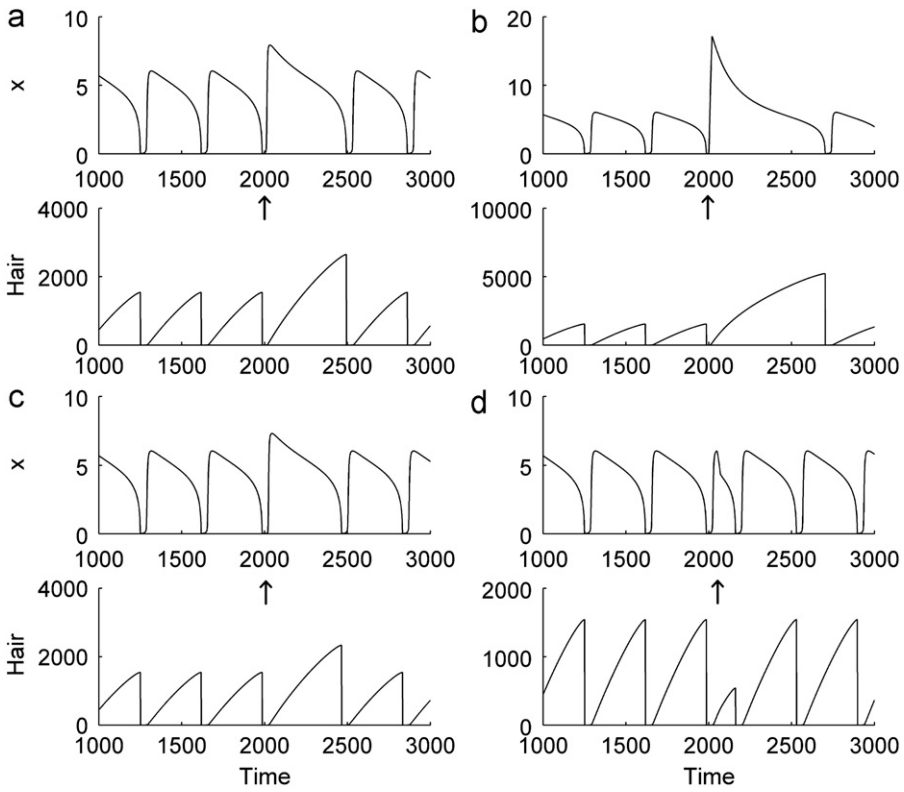

Fig. 10. Pulse perturbation time series of matrix keratinocytes and hair length. (a) Pulse in p_1 commencing at time $t=1995$, with a maximum value of $p_1=1.9$. (b) Pulse in parameter a commencing at time $t=1995$, with a maximum value of $a=1.9$, denoted by arrow. (c) and (d) Pulse perturbations of parameter p_4 (at $t=2100$, with amplitude maximum value of $p_4=1.9$) result in phase dependent effects with stimulation of a prolonged hair cycle if pulsed during telogen (c); or abrogation of anagen if pulsed during anagen (d). Pulse timing marked by arrows.

all parameters and find parameter p_1 to be the most sensitive in achieving the transition (i.e. inducing permanent oscillations with a minimum of relative change). For example, an 8.8% increase in p_1 is sufficient to achieve the transition. Parameter c requires only a slightly larger change (10%) to achieve permanent oscillations.

The fact that the lower fixed point loses stability in a subcritical Hopf bifurcation implies that it might be excitable in the monostable state (Fig. 5d, $p_1<0.415$), implying that a short pulse (treatment) could start a full cycle. The monostable state would be interpreted as a non-cycling hair (such as occurs in severe alopecia). To test this we apply a pulse perturbation in parameter p_1 to the system prepared in the no growth steady state outside of the bistable region. When the pulse is below a threshold, the effect of the stimulation is negligible and leads to a trivial damped oscillatory return to the no growth state. As such the perturbation can be considered ineffective. If, however, the pulse is suprathreshold as in Fig. 11b the model produces a large amplitude excursion with a similar period to the oscillatory solution (compare with Fig. 11a). The duration of the pulse was 5 time points, however longer pulses also produce a longer cycle. Therefore, the MK population is in an excitable condition and a comparatively moderate stimulus can induce one full cycle of the HF oscillation. After one cycle the system returns to the no growth fixed point and remains there, as it is the only stable solution. To maintain cyclical regeneration of hair growth, one must repeat the pulse once the MK population returns to the resting state. This is shown in Fig. 11c, where a regular pulse of appropriate frequency into the monostable no growth system (with $p_1=0.3$) induces "regular" cyclical behaviour. This uses the property that an excitable system performs the full cycle once induced by a suprathreshold stimulus. The period of this induced cyclical behaviour is less than the period in the autonomous cycling, mainly because the system is allowed to settle to the resting state before it is perturbed again. Comparing Figs. 11b and c it can be noted that the amplitude of the periodically pulsed system (Fig. 11c) is even slightly larger than the amplitude of the cycle in the single stimulus simulation (Fig. 11b). If induced regular cycling with full hair growth is desired, the period of the stimuli cannot be decreased below a certain minimum length as a stimulus during the cycle or at the beginning of the resting phase, when the system is refractory, does not lead to a full new cycle. The refractory period is divided in a phase of absolute refractoriness and a phase of relative refractoriness where a stimulus leads to a graded response. A smaller period than the one chosen in Fig. 11c (stimulating during the phase of relative refractoriness) leads to irregular hair growth with hairs of different length and decreased average hair length. Phenomena such as "missed beats" and induction of a full cycle for every second stimulus are observed in these cases.

4. Discussion and conclusion

The human HF exhibits a unique chronobiological rhythm known as the hair cycle. The molecular or cellular control mechanism(s) responsible for this regenerative process has not been identified. In this study, we have reviewed essential dynamical features of the human hair cycle follicle and presented a prototypic mathematical model to advance a theory of the human hair cycle. This model focuses on the dynamics of hair MK. We argue that a plausible feedback-control structure between two key compartments (MK and DP) leads to instabilities in the population dynamics resulting in rhythmic hair growth. The model proposes that the underlying oscillation consists of an autonomous

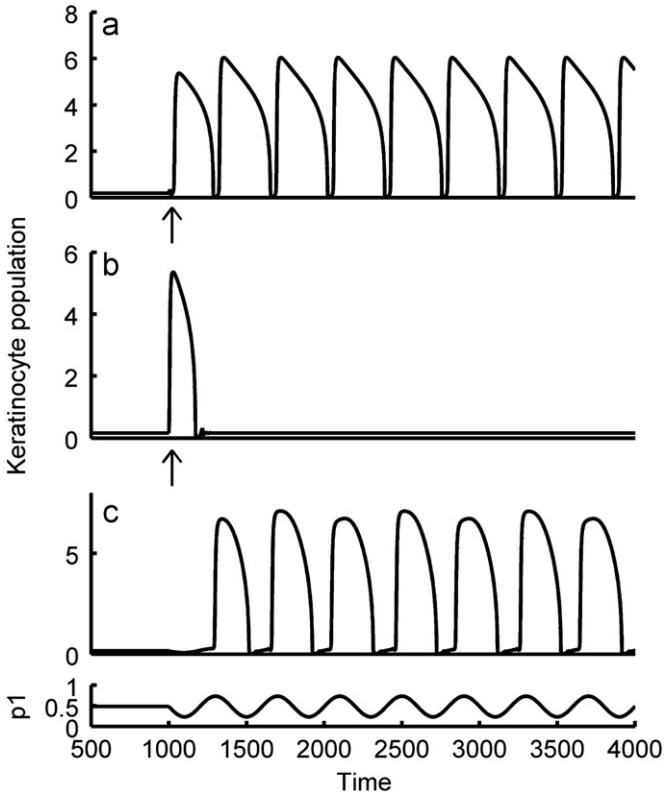

Fig. 11. The hair cycle model predicts possible mechanisms for the treatment of hair loss. (a) Switching from the lower steady state to the oscillatory state in the bistable region with single pulse in p_1. The pulse up to $p_1=0.49$ for 5 time point commencing at $t=1000$. (b) Pulse as in (a) but applied in the monostable region. No hair cycling (before pulse) may be perturbed into a whole hair cycle. (c) Periodic pulses to p_1 starting from $t=1000$ (bottom panel). Regular administered therapy achieves repeated cycling behaviour.

switching between two quasi-steady states. Additional features of the model, namely bistability and excitability, lead to new hypotheses about the impact of interventions on hair growth.

The model Eq. (4) was constructed from features regarding HF dynamics and interactions derived from the literature. These were incorporated into the model on the cell population level while specific molecular processes were purposely not included. However, the two compartment model (Fig. 4) opens the exploration of how human HF dynamics may arise from control processes governing the spatial scale of the multi-cellular MK population as a whole.

An important finding in our study is that neither feedback inhibition nor the presence of bistability alone is sufficient to explain the full dynamics of the HF. However, both have been postulated as mechanisms for the hair cycle. Concerning delayed feedback inhibition, Chase proposed that the hair cycle is based on an intrinsic inhibition–disinhibition switch (Chase, 1954). Even though this theory has been followed up by the delineation of several descriptive theories on the oscillatory nature of the HF as a result of delayed feedback inhibition (Paus et al., 1999; Stenn et al., 1999; Paus and Foitzik, 2004), none of these have led to a mathematical formalisation of HF cycling. However, the accumulation of inhibitory signals during anagen is supported by the finding that chalone-like inhibitory signals are indeed present during telogen in mouse skin, which are capable of inhibiting experimentally induced anagen development (Paus et al., 1990). Our new mathematical model supports this basic concept by showing that feedback inhibition allows the production of oscillations in MK numbers and the associated production of hair shafts. In our case, part of the delay in feedback arises from transport processes between the two compartments rather than biochemical reactions. This produces oscillations that are described mathematically as the result of a supercritical Hopf bifurcation. Although the frequency of these oscillations could be regulated to better fit the low frequency of the hair cycle via modulation of parameters in the feedback loop, we cannot assume the molecular processes (such as synthesis and diffusion) to be much slower than population growth and decay constants. Therefore, the resultant frequency of oscillations remains on a comparatively fast time scale in the absence of bistability ($k=1$). Importantly, it is unrealistic that feedback inhibition alone may account for the characteristic profile of the biological process as specified in Fig. 2. The reason for this is that a fast oscillating keratinocyte population would not clearly distinguish between durations of anagen, catagen and telogen phases in terms of periodicity as seen in vivo and therefore does not explain the asymmetric low frequency hair cycle profiles observed in human hair cycling.

It is known that a simple linear sequence of biochemical reactions can explicitly produce time delays (see e.g. Mocek et al., 2005). The impact of negative feedback modelled by a chain of linear (first-order) reaction terms on the systems dynamics is well-studied, for instance in the Goodwin model (Goodwin, 1963). As the delay mechanism in our model is also described by linear terms, the feedback control (for example of proliferation) can be expected to have similar impact on the population dynamics. As such the appearance of oscillatory solutions is not unexpected. The assumption of a feedback mechanism that involves transport between two spatially distinct compartments is a mechanism to realise a delay. This has been used previously to explain the onset of oscillatory behaviour in a different context (Hoffmann et al., 2002).

Interestingly, the presence of a dynamical bistability to explain the two main dynamic "states" (anagen and telogen) of the HF has been recently postulated but no mathematical model was provided (Bernard, 2012). Switching between the two states was proposed to be driven by random fluctuations. If we consider bistability alone as a possible mechanism for the hair cycle then this would imply that there is no continuous (monotonous) evolution towards the switching point. In reality, however, catagen HFs cannot transform back into anagen once they have started to enter catagen; instead, they have to proceed through telogen in order to re-enter anagen. This "quiescent" state appears to be important, e.g. for proper reactivation of HF epithelial stem cells in the bulge and secondary hair germ as a prerequisite for anagen development. This mandatory, non-reversible sequence of cyclic HF transformation events occurs both under physiological and pathological conditions, e.g. in response to chemotherapy (Hendrix et al., 2005). Therefore, in the in vivo situation different sub-phases of the hair cycle are defined with continuous evolution of morphological features (Kligman, 1959; Dawber, 1997; Kloepper et al., 2010). Therefore, if the mechanism of the hair cycle was to operate via bistability alone, the ability to produce the wide range of dynamics typically seen in the HF would be impossible to achieve.

Following these considerations, our theory of the hair cycle therefore requires both bistability and feedback inhibition to produce its key dynamical features. When both bistability and inhibitory feedback are present, cyclical switching occurs between a state of large population with strong growth (anagen), and a subsequent state of near-zero population with no growth (telogen). Anagen is explained as a period in which the proliferation rate and the apoptotic rate change continuously but at two time scales: one in which proliferation dominates over apoptosis such that the population level rises and one in which apoptosis dominates over proliferation and the population level falls. The

slow decrease of the MK population during anagen is due to slow accumulation of the inhibitory feedback species. It continues until a threshold is reached and apoptotic processes take over so the decrease accelerates leading to catagen. The rapid decrease of the keratinocyte population results in abrogation of hair growth. The period of relative quiescence (telogen) then maintains the near-zero population while the impact of the inhibitory species slowly decreases until a second threshold is reached and a new cycle starts leading to the creation and growth of a new hair. Thus, the crucial prerequisite for the switching mechanism is the combination of a bistability between a state of rapid growth and a no growth state with a cyclical process. Autonomous cycling between two pseudo-steady states yields the observed switching. As described earlier, the accumulation of inhibitory signals during anagen is described in previously postulated theories (Chase, 1954; Paus et al., 1999; Stenn et al., 1999; Paus and Foitzik, 2004), and it has been demonstrated experimentally that inhibitory signals are present during telogen in mouse skin (Paus et al., 1990).

The model relies on several assumptions that require critical assessment. Firstly, we assume that the behaviour of interest resides at the level of groups of cells; i.e. in the cyclical regeneration of epithelial HF compartments during the hair cycle and in the observation of hair shaft growth. Thus, macroscopic cell population considerations form the basis of our theoretical treatment of the HF cycle. Indeed, important processes will be involved at multiple scales and, in particular, molecular interactions that are often the subject of experimental investigations into the hair cycle will be described on the microscopic scale. In the model presented here we consider the high level of processes that may govern the whole cells and populations of cells. This is in line with a current model of interacting populations of HF stem cells in mice (Plikus et al., 2011) and also with the initial dynamical hypothesis of (Chase, 1954). Future modelling work will address the multi-scale mechanisms of HF cycling and will make more specific predictions regarding exact numbers of cells involved in the modelled processes. An important step will be to identify candidates for the signalling morphogens. Morphogen z, for example, is produced in the DP and acts in the matrix. Therefore two reasonable candidates are noggin, which acts on the BMP signalling pathway (Botchkarev et al., 1999) or HGF, which is a DP specific secreted growth factor whose receptor (c-Met) is expressed in the epithelial bulb (i.e. the matrix) (Jindo et al., 1995, 1998; Lindner et al., 2000).

Secondly, our population level approach focuses on the cells arising from epithelial stem cells that best embody the dynamic changes in HF structure and are directly responsible for hair growth during anagen, namely the MKs. Therefore, we assume that if we understand the controls governing the cyclical regeneration and regression of the MKs then we can understand the hair cycle mechanism. This is justified as the MK population, at numbers close to zero, is likely to capture the epithelial progenitor populations that derive from bulge stem cells and eventually differentiate into MKs. For simplicity and to emphasise key dynamic components, we did not explicitly differentiate between these cell types. Similarly, we assumed a simplified constant input of stem cells to the MK population. Biologically, it is evident that the system is more complicated than our assumptions account for and we envisage future models to encompass processes on a multi-scale level. Despite the simplifications made, we have managed to account for a great amount of hair cycling or HF dynamic phenomena.

Thirdly, we assume the process of the human hair cycle is autonomous. This is not only supported by long-appreciated clinical and experimental evidence arising from, for example, human hair transplantation and HF organ culture as described earlier, but also by the recent landmark work of Plikus et al. who predict the human HF to rely heavily on intrinsic processes in order to cycle (Plikus et al., 2011). This inherent autonomy does not detract from the fact that the human HF is sensitive to a multitude of extrafollicular growth-modulatory influences (Paus and Cotsarelis, 1999; Schneider et al., 2009), which all can impact on the model proposed here. A more complete description of human HF cycling will eventually incorporate the influences of both intra- and inter-follicular processes. Clearly the former, as proposed in the current study are crucial to this multi-scale endeavour.

In this model, we are able to observe the strong asymmetry between stage lengths in the human hair cycle caused by the vicinity of a saddle-node on limit cycle bifurcation that leads to slowing down of the anagen phase but not of telogen. The model thus offers an explanation for the unique periodicity of each phase of the hair cycle whereby human scalp hair can grow for some years before it sheds while telogen is typically of the order of a few months. The previously postulated theories of hair cycling do not address how this salient feature may arise.

Despite the abstraction of the hair biology involved the simplistic model proposed here is able to capture the wide variation in dynamics exhibited by the HF and successfully addresses a large proportion of features that are thought essential to a successful theory of the hair cycle (Paus and Foitzik, 2004). The model produces unique asymmetric phases of the hair cycle, and a hair shaft output, as an autonomous process and additionally accounts for varied hair cycle lengths which is dependent on parameter values. Additionally, the model provides some predictions of how hair disorders such as miniaturisation of the HF and severe cases of "no growth" behaviour may arise. We show that the hair cycle and resultant hair may be different lengths by altering parameter values. These parameter differences may reflect the intrinsic properties of HFs located in different body regions or between individuals. This leads to the hypothesis that the intrinsic properties in HFs from one body region to the next (represented by variation in parameters such as p_1) are the cause of the different hair lengths seen in vivo, for example between eyebrow and scalp hairs. This is also in line with the accepted concept that the HF mesenchyme dictates the region-specific phenotype of a HF. Our model incorporates the mesenchymal compartment (DP) as an intrinsically important component of the hair cycling process (Hardy, 1992; Ohyama et al., 2010).

Within the present framework, cycle to cycle variation may be accounted for by random fluctuations in model parameters. Great changes in hair cycle duration and hair growth can occur from one cycle to the next (Tobin et al., 2003, Courtois et al., 1994). This can be interpreted as variations of the period (and amplitude) of an autonomous cycling process due to environmental perturbations. In addition, we briefly studied how fluctuations in the lengths of anagen, catagen and telogen from one cycle to the next can be achieved by introducing random fluctuations in the input (supply from stem cells (a)) to the MKs and in the strength of activation of growth of these cells (p_1) (Supplemental Figs. 1 and 2). Random fluctuations in stem cells and p_1 together seem to be important factors in the model, but for a future sensitivity analysis (to determine the processes that contribute strongest to the variability), estimates of the degree of fluctuations in each parameter are required. This gives a new account of the data presented in relation to the follicular automaton model, which suggests that the hair cycle is a stochastic switching process assuming two underlying stable states but not an autonomous cycling process (Halloy et al., 2000, 2002). A more thorough examination of the role of stochastic effects in the current model, including the influence of noise strength, will be an interesting topic for future investigation.

As hair disorders are the result of a pathological alteration in normal hair cycle dynamics, the model allows us to capture not only normal variation in hair cycling behaviour, but also that of hair pathologies. The most common of these is androgenetic alopecia (pattern baldness) which is characterised by the miniaturisation of the HF, shortening of the hair cycle and diminution of visible hair. This model provides several predictions to explain how these changes may arise. The opposite transition occurs in hirsutism whereby there is an increase in hair cycle length and hair size. For example, timed perturbation (e.g. increase in p_1) of a short cycling HF can produce a longer hair cycle (Fig. 10a) and the opposite is a possible mechanism for the terminal to vellus transition seen in pattern baldness (i.e. decrease in parameter such as p_1). The results of these perturbations are occasionally non-intuitive but can be explained from the bifurcation and phase space structure of the model. This suggests that candidate molecules which directly impact on the proliferation rate of the MK can be used for perturbation experiments. In addition, our study specifically predicts that the response of the hair follicle to addition of apoptotic effectors is phase-dependent. This can be experimentally verified by pulse treatment of hair follicles in vitro, for which there are well defined staging methods available (Kloepper et al., 2010).

The model predicts, firstly, in the bistable situation where the no growth state coexists with the periodic hair cycling that there are possibilities of inducing regular cycling from the no growth state by applying a single, comparatively brief stimulus. Similarly, a single comparatively brief stimulus would be sufficient to switch the process from cyclical growth to no growth. In either case the minimum strength of the perturbation to achieve the transition depends on the critical population size as defined by the separating manifold.

This result would predict the possibility that a normally cycling HF could switch to a "permanently" non-cycling follicle due to an accidental environmental stimulus if it is in this particular bistable state. This is a new hypothesis to explain the transition from growth to no growth that occurs in conditions such as severe alopecia or in chemotherapy induced alopecia. The model also predicts that there might be effective treatments to cure this problem. Secondly, for the situation where there is a single stable state of no growth, such as may occur in advanced androgenetic alopecia (Cotsarelis and Millar, 2001), the model predicts that there is a potential way to cure. We predict that the HF exhibits the dynamical property of excitability. Excitability is a generic feature in the subthreshold vicinity of Hopf bifurcations. If the HF is in an excitable state (near the fold of limit cycle bifurcation in Fig. 5d), a short pulse (treatment) could start a full cycle. Of course the success of this intervention depends on whether the other model assumptions are fulfilled including, for example, sufficient supply from the bulge stem cells. Indeed, it has recently been shown that androgenetic alopecia arises from the lack of activation of stem cells rather than from the depletion of stem cell number, therefore, the assumption of stem cell supply as proposed here may be fulfilled (Garza et al., 2011). In addition, in advanced alopecia a prolonged telogen phase may be observed (Dawber, 1997; Cotsarelis and Millar, 2001). Our model postulates that this prolonged telogen phase may be explained by the HF being in the lower steady state in the bistable region (see Fig. 11) with the presence of a time delay for the stimulus to the HF to overcome the threshold and enter a full cycle. This would produce a long telogen phase until the HF is then stimulated above the threshold to then enter the anagen phase again. Lacking a detailed quantitative model the threshold would have to be determined empirically, however, the model provides first hints as to which parameter(s) might be suitable and may guide us in the means to realise the perturbation.

The notion of HF excitability being an important feature in the dynamics of hair cycling is also reflected in Plikus et al. but at a higher spatio-temporal level (Plikus et al., 2011). The excitable state of our model offers an alternative possibility for cycling whereby successive activations are driven by suprathreshold excitation, causing a single cycle. Alongside parametric noise, this is an alternative way to explain the variation seen in telogen stages, whereby the timing of extrinsic activations is stochastic.

If the goal of treatment is to maintain a cyclical hair growth in a single follicle under the excitable condition, it is necessary to apply appropriately timed periodic stimuli. In particular, at the end of catagen there is a refractory period during which a brief perturbation does not induce a new cycle (absolute refractoriness) or induces only a short cycle of small amplitude implying a short hair (relative refractoriness). The notion of refractory telogen had been postulated many years ago and the concept was recently supported via experimental work (Plikus et al., 2008, 2011). Loosely speaking, their term 'refractory telogen' and 'competent telogen' could be viewed as equivalent to absolute refractoriness and relative refractoriness respectively. However, the terms used by Plikus et al. refers to the interaction between neighbouring follicles rather than the excitability of the HF itself. Our model further develops this concept in the dynamic behaviour of the single HF. In the future, this modelling approach may be used to dissect the seemingly complex interactions and roles of factors in the hair cycle to better understand its mechanisms an improve our approach to treating hair cycling abnormalities (Cotsarelis and Millar, 2001; Al-Nuaimi et al., 2010).

A major limitation of the current study is the use of arbitrary parameters. The reason for working with arbitrary parameters is that the model is reduced so as to facilitate conceptualisation of the hair cycle in terms of dynamics and to implement a theory of the process. The abstraction employed here means that there is a lack of experimental data at this higher level. The parameters used in this current model are likely to therefore represent "lumped" parameters. One evident challenge therefore is to now dissect the individual components of these "lumped" parameters and their relative impact on the behaviour of the model.

The use of multi-scale modelling would allow experimental data at the molecular level to marry with tissue level processes that encapsulate the hair cycle. Now that we have studied macroscopic properties of the system, we are able to build upon a directed experimental approach. Biologically, an essential component in the hair cycle is the spatial interaction between compartments; in particular, bidirectional communication between the keratinocyte population and the DP. We implemented a two-compartment model assuming two (molecular) species to be involved in the communication. The communication process mathematically represents a feedback loop via coupling of compartments. Possible biological candidates include molecules that are known to diffuse between the DP and the hair matrix such as those interacting in SHH, WNT, BMP and TGF-β signalling (Botchkarev and Kishimoto, 2003; Schneider et al., 2009; Plikus et al., 2009; Oshimori and Fuchs, 2012).

Autonomy is a pronounced feature of the human HF. This is demonstrated by the shedding of individual hairs rather than synchronised shedding and is a result of the population of HFs following an asynchronous cycle in relation to each other, thus generating the characteristic mosaic pattern of human HF cycling. This does not however, exclude communication between human HFs. For example, in other mammals, such as mice, the HFs exhibit more synchronised cycling behaviour which results in a patch of hair simultaneously growing or shedding. In the recent model of communication between stem cells in HFs, the waves of synchronised cycling were explained by abstract coupling between HF stem cells (Plikus et al., 2011). This coupling is

mediated by the diffusion of activators and inhibitors with the WNT and BMP signalling pathways confirmed as contributing to this communication. In addition fibroblast growth factor (FGF), and transforming growth factor (TGF)-β signalling pathways have also been implicated in follicular activation and inhibition (Plikus, 2012). It was suggested that an increase of inhibitory signalling could explain reduced synchronisation in human HF stem cells. Such a mechanism could be implemented in our model by diffusive coupling of variables z between HF compartments.

At present there appears to be no direct evidence for the type or level of communication between human HFs. However, the possibility remains that in certain human hair disorders the degree of communication between human HFs may lead to simultaneous shedding of a population of HFs. Since human HFs appear to cycle in a fairly synchronised manner *in utero* and immediately after birth and can be partially resynchonised for example by a number of endocrinological abnormalities in adult life (Dawber, 1997; Paus and Foitzik, 2004), it is reasonable to assume that interfollicular communication along the lines dissected by Plikus et al. for the mouse also occurs between human HFs. Therefore, this communication between human HFs may underlie the simultaneous hair shaft shedding in defined collectives of human HF populations, such as during telogen effluvium or excessive exogen (Paus, 2006; Higgins et al., 2009). If confirmed, again the current model could help to describe this phenomenon mathematically.

Since previously proposed theories of the hair cycle were verbally expressed and not tested mathematically the present model is an advance from the important work of previous hair biologists (Chase, 1954; Sun et al., 1991; Paus et al., 1999; Stenn et al., 1999; Paus and Foitzik, 2004). Likewise, previous mathematical models concerned with hair growth and cycling do not address the intrinsic processes that drive the HF through the cycle (Halloy et al., 2000, 2002; Plikus et al., 2011). The mathematical model by Plikus et al. addresses the mechanism of HF coupling in the propagation of hair cycle waves in mice and other mammals and is therefore at a higher level of interest (Plikus et al., 2011). Importantly, Plikus et al. show that uncoupling of stem cell interactions between neighbouring HFs produces the independent HF cycling seen in adult human HFs and postulate that alopecia may arise by the reduction of activation of stem cells. The model does not explore what the internal mechanisms may be in the human case (Plikus et al., 2011). Our model, by focusing on the internal mechanism, thus instructively complements previously proposed hair cycle theories.

The current model can now be utilised for *in silico* modelling of hair growth modulators within this dynamical systems framework. This will enable the better delineation of the effects of well-known and novel modulators of the hair cycle. For example, growth factors that are considered to induce growth and proliferation (because they prolong anagen) may in reality act as inhibitors. As shown in this study an inhibitory effect in our model is predicted to be required at some level to maintain the long growth phase. This may explain why experiments can produce conflicting results depending on their outcome measurements and timing of interventions. This model also predicts that the phase of intervention is critical for producing the particular result obtained following certain perturbations.

The hair cycle is a complex process involving multi-scale coordination of events. Mathematical modelling promises to help dissect the intricacies of this system (Al-Nuaimi et al., 2010). The novel theory proposed here is that the human hair cycle requires two key dynamical features; feedback inhibition and a bistable switch and represents a new approach to deciphering the core components that drive the hair cycle using mathematical modelling.

In addition, our model predicts that the response of hair growth disorders to treatment critically depends on the bistability and excitability of the HF and on the extent to which these components of HF behaviour have been reversibly or irreversibly altered. Therefore, the current mathematical model is not only capable of paving the way to better understand and predict the dynamic properties of the human HF, but can also define novel targets for therapeutic interventions and more effective hair growth-modulatory agents.

Acknowledgements

YA and MG acknowledge EPSRC and BBSRC for funding via the Doctoral Training Centre in Integrative Systems Biology. MG also acknowledges support from the EPSRC via a post-doctoral prize at the University of Manchester. RP acknowledges the Manchester Academic Health Sciences Centre. GB acknowledges EPSRC and BBSRC for financial support.

Appendix A. Supplementary material

Supplementary data associated with this article can be found in the online version at http://dx.doi.org/10.1016/j.jtbi.2012.05.027.

References

Al-Nuaimi, Y., Baier, G., et al., 2010. The cycling hair follicle as an ideal systems biology research model. Exp. Dermatol. 19 (8), 707–713.
Bernard, B.A., 2012. The hair follicle, a bistable organ. Exp. Dermatol. 21 (6), 401–403.
Bodó, E., Kany, B., et al., 2010. Thyroid-stimulating hormone, a novel, locally produced modulator of human epidermal functions, is regulated by thyrotropin-releasing hormone and thyroid hormones. Endocrinology 151 (4), 1633–1642.
Botchkarev, V.A., Botchkareva, N.V., et al., 1999. Noggin is a mesenchymally derived stimulator of hair-follicle induction. Nat. Cell Biol. 1 (3), 158–164.
Botchkarev, V.A., Kishimoto, J., 2003. Molecular control of epithelial–mesenchymal interactions during hair follicle cycling. J. Invest. Dermatol. Symp. Proc. 8, 46–55.
Chase, H.B., 1954. Growth of the hair. Physiol. Rev. 34, 113–126.
Cotsarelis, G., Millar, S.E., 2001. Towards a molecular understanding of hair loss and its treatment. Trends Mol. Med. 7 (7), 293–301.
Cotsarelis, G., 2006. Epithelial stem cells: a folliculocentric view. J. Invest. Dermatol. 126, 1459–1468.
Courtois, M., Loussouam, G., et al., 1994. Hair cycle and alopecia. Skin Pharmacol. 7 (1-2), 84–89.
Dawber, R. (Ed.), 1997. Diseases of the Hair and Scalp. Blackwells, Oxford.
Garza, L.A., Yang, C.-C., et al., 2011. Bald scalp in men with androgenetic alopecia retains hair follicle stem cells but lacks CD200-rich and CD34-positive hair progenitor cells. J. Clin. Invest. 121 (2), 613–622.
Geyfman, M., Andersen, B., 2010. Clock genes, hair growth and aging. Aging 2 (3), 122–128.
Golichenkova, P.D., Doronin, Y.K., 2008. Reconstruction of proliferative activity of hair follicle cells based on the geometric parameters of the hair shaft. Moscow Univ. Biol. Sci. Bull. 632 (2), 77–79.
Goodwin, B.C., 1963. Temporal Organization of Cells. Academic Press, New York.
Greco, V., Chen, T., et al., 2009. A two-step mechanism for stem cell activation during hair regeneration. Cell Stem Cell 4, 155–169.
Halloy, J., Bernard, B.A., et al., 2000. Modeling the dynamics of human hair cycles by a follicular automaton. Proc. Natl. Acad. Sci. USA 97 (15), 8328–8333.
Halloy, J., Bernard, B.A., et al., 2002. The follicular automaton model: effect of stochasticity and of synchronization of hair cycles. J. Theor. Biol. 214 (3), 469–479.
Hardy, M.H., 1992. The secret life of the hair follicle. Trends Genet. 8 (2), 55–61.
Harries, M.J., Paus, R., 2010. The pathogenesis of primary cicatricial alopecias. Am. J. Pathol. 177 (5), 2152–2162.
Hendrix, S., Handjiski, B., et al., 2005. A guide to assessing damage response pathways of the hair follicle: lessons from cyclophosphamide-induced alopecia in mice. J. Invest. Dermatol. 125 (1), 42–51.
Higgins, C.A., Westgate, G.E., et al., 2009. From telogen to exogen: mechanisms underlying formation and subsequent loss of the hair club fiber. J. Invest. Dermatol. 129, 2100–2108.

Hoffman, A., Levchenko, A., et al., 2002. The IκB–NF–κB signaling module: temporal control and selective gene activation. Science 298 (5596), 1241–1245.
Hsu, Y.C., Pasolli, H.A., et al., 2011. Dynamics between stem cells, niche, and progeny in the hair follicle. Cell 144 (1), 92–105.
Ibrahim, L., Wright, E.A., 1982. A quantitative study of hair growth using mouse and rat vibrissal follicles. J. Embryol. Exp. Morphol. 72, 209–224.
Ito, M., Kizawa, K., et al., 2004. Hair follicle stem cells in the lower bulge form the secondary germ, a biochemically distinct but functionally equivalent progenitor cell population, at the termination of catagen. Differentiation 72 (9–10), 548–557.
Jindo, T., Tsuboi, R., et al., 1995. The effect of hepatocyte growth factor/scatter factor on human hair follicle growth. J. Dermatol. Sci. 10 (3), 229–232.
Jindo, T., Tsuboi, R., et al., 1998. Local injection of hepatocyte growth factor/scatter factor (HGF/SF) alters cyclic growth of murine hair follicles. J. Invest. Dermatol. 110 (4), 338–342.
Kligman, A.M., 1959. The human hair cycle. J. Invest. Dermatol., 307–316.
Kloepper, J.K., Sugawara, K., et al., 2010. Methods in hair research: how to objectively distinguish between anagen and catagen in human hair follicle organ culture. Exp. Dermatol. 19 (3), 305–312.
Kolinko, V., Littler, C.M., 2000. Mathematical modeling for the prediction and optimization of laser hair removal. Lasers Surg. Med. 26 (2), 164–176.
Kwon, O.S., Oh, J.K., et al., 2006. Human hair growth ex vivo is correlated with in vivo hair growth: selective categorization of hair follicles for more reliable hair follicle organ culture. Arch. Dermatol. Res. 297 (8), 367–371.
Lavker, R.M., Sun, T.T., et al., 2003. Hair follicle stem cells. J. Invest. Dermatol. Symp. Proc. 8 (1), 28–38.
Levy, V., Lindon, C., et al., 2005. Distinct stem cell populations regenerate the follicle and interfollicular epidermis. Dev. Cell 9 (6), 855–861.
Lindner, G., Botchkarev, V.A., et al., 1997. Analysis of apoptosis during hair follicle regression (catagen). Am. J. Pathol. 151 (6), 1601–1617.
Lindner, G., Menrad, A., et al., 2000. Involvement of hepatocyte growth factor/scatter factor and met receptor signaling in hair follicle morphogenesis and cycling. FASEB J. 14 (2), 319–332.
Link, R.E., Paus, R., et al., 1990. Epithelial growth by rat vibrissae follicles in vitro requires mesenchymal contact via native extracellular matrix. J. Invest. Dermatol. 95 (2), 202–207.
Matsuo, K., Mori, O., et al., 1998. Apoptosis in murine hair follicles during catagen regression. Arch. Dermatol. Res. 290, 133–136.
Matsuzaki, T., Yoshizato, K., 1998. Role of hair papilla cells on induction and regeneration processes of hair follicles. Wound Repair Regen. 6 (6), 526–530.
Milner, Y., Sudnik, J., et al., 2002. Exogen, shedding phase of the hair growth cycle: characterization of a mouse model. J. Invest. Dermatol. 119, 639–644.
Mocek, W.T., Rudnicki, R., et al., 2005. Approximation of delays in biochemical systems. Math. Biosci. 198, 190–216.
Nagorcka, B.N., Mooney, J.R., 1982. The role of a reaction-diffusion system in the formation of hair fibres. J. Theor. Biol. 98 (4), 575–607.
Nutbrown, M., Randall, V.A., 1995. Differences between connective tissue-epithelial junctions in human skin and the anagen hair follicle. J. Invest. Dermatol. 104, 90–94.
Ohyama, M., Zheng, Y., et al., 2010. The mesenchymal component of hair follicle neogenesis: background, methods and molecular characterization. Exp. Dermatol. 19 (2), 89–99.
Oshimori, N., Fuchs, E., 2012. Paracrine TGF-β signaling counterbalances BMP-mediated repression in hair follicle stem cell activation. Cell Stem Cell 10 (1), 63–75.
Panteleyev, A.A., Botchkareva, N.V., et al., 1999. The role of the hairless (*hr*) gene in the regulation of hair follicle catagen transformation. Am. J. Pathol. 155 (1), 159–171.
Panteleyev, A.A., Jahoda, C.A.B., et al., 2001. Hair follicle predetermination. J. Cell Sci. 114 (9), 3419–3431.
Paus, R., 2006. Therapeutic strategies for treating hair loss. Drug Discov. Today 3 (1), 101–110.
Paus, R., Cotsarelis, G., 1999. The biology of hair follicles. N. Engl. J. Med. 341, 491–497.
Paus, R., Foitzik, K., 2004. In search of the "hair cycle clock": a guided tour. Differentiation 72, 489–511.
Paus, R., Muller-Rover, S., et al., 1999. Chronobiology of the hair follicle: hunting the "hair cycle clock". J. Invest. Dermatol. Symp. Proc. 4 (3), 338–345.
Paus, R., Stenn, K.S., et al., 1990. Telogen skin contains an inhibitor of hair growth. Br. J. Dermatol. 122 (6), 777–784.
Philpott, M.P., Green, M.R., et al., 1990. Human hair growth in vitro. J. Cell Sci. 97, 463–471.
Plikus, M.V., Baker, R.E., et al., 2011. Self-organizing and stochastic behaviors during the regeneration of hair stem cells. Science 332, 586–589.
Plikus, M.V., Mayer, J.A., et al., 2008. Cyclic dermal BMP signalling regulates stem cell activation during hair regeneration. Nature 451 (7176), 340–344.
Plikus, M.V., Widelitz, R.B., et al., 2009. Analyses of regenerative wave patterns in adult hair follicle populations reveal macro-environmental regulation of stem cell activity. Int. J. Dev. Biol. 53, 857–868.
Plikus, M.V., 2012. New activators and inhibitors in the hair cycle clock: targeting stem cells' state of competence. J. Invest. Dermatol. 132 (5), 1321–1324.
Saitoh, M., Uzuka, M., et al., 1970. Human hair cycle. J. Invest. Dermatol. 54 (1), 65–81.
Schneider, M.R., Schmidt-Ullrich, R., et al., 2009. The Hair follicle as a dynamic miniorgan. Curr. Biol. 19 (3), R132–R142.
Slominski, A., Wortsman, J., et al., 2005. Hair follicle pigmentation. J. Invest. Dermatol. Symp. Proc. 124, 13–21.
Soma, T., Ogo, M., et al., 1998. Analysis of apoptotic cell death in human hair follicles in vivo and in vitro. J. Invest. Dermatol. 111 (6), 948–954.
Stenn, K.S., Nixon, A.J., et al., 1999. What controls hair follicle cycling? Exp. Dermatol. 8, 229–236.
Stenn, K.S., Paus, R., 2001. Controls of hair follicle cycling. Physiol. Rev. 81 (1), 449–494.
Stenn, K.S., Prouty, S.M., et al., 1994. Molecules of the cycling hair follicle—a tabulated review. J. Dermatol. Sci. 7 (Suppl.), S109–S124.
Sun, T.T., Cotsarelis, G., et al., 1991. Hair follicular stem cells: the bulge activation hypothesis. J. Invest. Dermatol. 96 (5), 77s–78s.
Taylor, G., Lehrer, M.S., et al., 2000. Involvement of follicular stem cells in forming not only the follicle but also the epidermis. Cell 102, 451–461.
Tobin, D.J., 2011. The cell biology of human hair follicle pigmentation. Pigm. Cell Melanoma Res. 24, 75–88.
Tobin, D.J., Gunin, A., et al., 2003. Plasticity and cytokinetic dynamics of the hair follicle mesenchyme: implications for hair growth control. J. Invest. Dermatol. 120 (6), 895–904.
Tobin, D.J., Hagen, E., et al., 1998. Do hair bulb melanocytes undergo apoptosis during hair follicle regression (catagen)? J. Invest. Dermatol. 111 (6), 941–947.
Tyson, J.J., 2002. Biochemical oscillations. In: Fall, C.P., Marland, E.S., Wagner, J.M., Tyson, J.J. (Eds.), Computational Cell Biology. Springer, New York. (Chapter 9).
Unger, W.P., 2005. Hair transplantation: current concepts and techniques. J. Investig. Dermatol. Symp. Proc. 10 (3), 225–229.
Waghmare, S.K., Bansal, R., et al., 2008. Quantitative proliferation dynamics and random chromosome segregation of hair follicle stem cells. EMBO J. 27, 1309–1320.
Wilson, C., Cotsarelis, G., et al., 1994. Cells within the bulge region of mouse hair follicle transiently proliferate during early anagen: heterogeneity and functional differences of various hair cycles. Differentiation 55, 127–136.
Yang, C.-C., Cotsarelis, G., 2010. Review of hair follicle dermal cells. J. Dermatol. Sci. 57, 2–11.
Zhang, Y.V., Cheong, J., et al., 2009. Distinct self-renewal and differentiation phases in the niche of infrequently dividing hair follicle stem cells. Cell Stem Cell 5, 267–278.
Zhang, Y.V., White, B.S., et al., 2010. Stem cell dynamics in mouse hair follicles. Cell Cycle 9 (8), 1504–1510.